Accepted Manuscript

Diphenylurea derivatives for combating methicillin- and vancomycin-resistant *Staphylococcus aureus*

Ibrahim E. Hassan, Haroon Mohammad, Omar A. Qassem, Waleed Younis, Tamer M. Abdelghany, Ahmed Elshafeey, Mahmoud M. Abd Rabo Moustafa, Mohamed N. Seleem, Abdelrahman S. Mayhoub

PII: S0223-5234(17)30117-4

DOI: 10.1016/j.ejmech.2017.02.044

Reference: EJMECH 9240

To appear in: *European Journal of Medicinal Chemistry*

Received Date: 16 December 2016

Revised Date: 13 February 2017

Accepted Date: 17 February 2017

Please cite this article as: I.E. Hassan, H. Mohammad, O.A. Qassem, W. Younis, T.M. Abdelghany, A. Elshafeey, M.M. Abd Rabo Moustafa, M.N. Seleem, A.S. Mayhoub, Diphenylurea derivatives for combating methicillin- and vancomycin-resistant *Staphylococcus aureus*, *European Journal of Medicinal Chemistry* (2017), doi: 10.1016/j.ejmech.2017.02.044.

Graphical Abstract

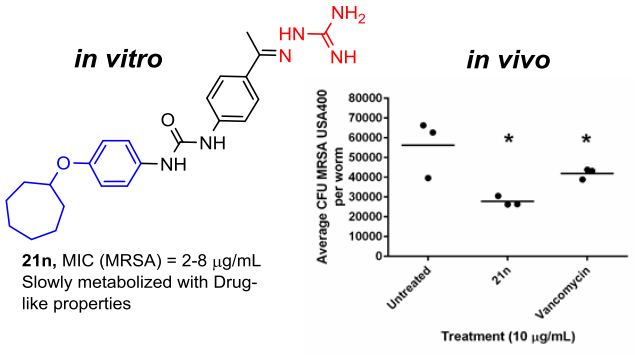

Diphenylurea Derivatives for Combating Methicillin- and Vancomycin-Resistant *Staphylococcus aureus*

Ibrahim E. Hassan,[a,‖] Haroon Mohammad,[b,‖] Omar A. Qassem,[a] Waleed Younis,[b] Tamer M. Abdelghany,[c] Ahmed Elshafeey,[d,e] Mahmoud M. Abd Rabo Moustafa,[f] Mohamed N. Seleem,[b,g *] and Abdelrahman S. Mayhoub[a,h*]

[a.] Department of Pharmaceutical Organic Chemistry, College of Pharmacy, Al-Azhar University, Cairo 11884, Egypt.

[b.] Department of Comparative Pathobiology, Purdue University, College of Veterinary Medicine, West Lafayette, IN 47907, USA.

[c.] Department of Pharmacology, College of Pharmacy, Al-Azhar University, Cairo 11884, Egypt

[d.] Department of Pharmaceutics, College of Pharmacy, Cairo University, Cairo 11777, Egypt.

[e.] Bioequivalence Section, Genuine Research Center, Heliopolis, Cairo 11757, Egypt.

[f.] Department of Pharmaceutical Chemistry, College of Clinical Pharmacy, University of Dammam, Eastern Province, KSA, P.O. Box 1982, Dammam 31441.

[g.] Purdue Institute for Inflammation, Immunology, and Infectious Diseases, West Lafayette, IN 479067, USA.

[h.] Biomedical Sciences, University of Science and Technology, Zewail City of Science and Technology, Giza, Egypt

Corresponding Authors.

* ASM; e-mail, amayhoub@azhar.edu.eg

* MNS; e-mail, mseleem@purdue.edu

Abbreviations. AMR, Antimicrobial resistance; Caco-2, heterogeneous human epithelial colorectal adenocarcinoma cells; CFUs, colony forming units; C_{max}, maximum serum concentration; HaCaT, human keratinocytes; MRT, mean residence time; P_{app}, apparent permeability; VISA, vancomycin-intermediate *S. aureus*.

Abstract. A new class of diphenylurea was identified as a novel antibacterial scaffold with an antibacterial spectrum that includes highly resistant staphylococcal isolates, namely methicillin- and vancomycin-resistant *Staphylococcus aureus* (MRSA & VRSA). Starting with a lead compound **3** that carries an aminoguanidine functionality from one side and a *n*-butyl moiety on the other ring, several analogues were prepared. Considering the pharmacokinetic parameters as a key factor in structural optimization, the structure-activity-relationships (SARs) at the lipophilic side chain were rigorously examined leading to the discovery of the cycloheptyloxyl analogue **21n** as a potential drug-candidate. This compound has several notable advantages over vancomycin and linezolid including rapid killing kinetics against MRSA and the ability to target and reduce the burden of MRSA harboring inside immune cells (macrophages). Furthermore, the potent anti-MRSA activity of **21n** was confirmed *in vivo* using a *Caenorhabditis elegans* animal model. The present study provides a foundation for further development of diphenylurea compounds as potential therapeutic agents to address the burgeoning challenge of bacterial resistance to antibiotics.

Keywords: antibiotic drug resistance, *Caenorhabditis elegans*, Methicillin-resistant *Staphylococcus aureus*, MRSA, intracellular infection, pharmacokinetics.

1. INTRODUCTION

Antimicrobial resistance (AMR) is a major global health concern. Recent alarming estimates suggest that deaths due to AMR may increase from the current estimate of 700,000 lives per year to ten million lives annually by 2050, at a cost of US$100 trillion.[1, 2] Different bacterial species that were once susceptible to several different classes of antibiotics have now acquired an array of unique resistance mechanisms. For instance, several strains of *Escherichia coli* were recently found to be resistant to the 3rd and 4th generation carbapenems[3] as well as the agent of last resort, colistin.[4] However, infections caused by one notorious bacterial pathogen have proven especially difficult to treat. Out of more than 23,000 people that die each year in the United States due to antibiotic-resistant bacterial infections,[5] methicillin-resistant *Staphylococcus aureus* (MRSA) was found to be responsible for nearly half of these fatalities. MRSA was first isolated in 1961,[6, 7] and became endemic in US hospitals in mid-1980, leading to the worldwide pandemic of MRSA that continues to the present time.[8, 9]

Staphylococcus aureus is a leading source of skin, wound, and hospital-acquired infections. Successful treatment of these infections has become a daunting challenge with the emergence of clinical isolates of MRSA exhibiting resistance to first-line antibiotics and agents of last resort, like linezolid[10] and vancomycin.[11] Furthermore, the effectiveness of agents of last resort (vancomycin) is limited by prolonged, persistent or recurrent bacteraemia during therapy,[12, 13] high rates of clinical failures,[14] severe nephrotoxicity[15] and the increasing prevalence of non-susceptible strains.[16] This highlights the urgent need to develop new therapeutic agents with novel scaffolds to address the burden of MRSA infections.

Our research group has been engaged extensively in developing and characterizing novel anti-MRSA compounds with the aim of discovering promising drug candidates.[17-21] Central to our vision of the urgent need to foster the current choices for the treatment of highly-resistant pathogens, we continued our intensive efforts to introduce new anti-MRSA scaffold(s) to the medicinal chemistry community. As reported earlier, the anti-MRSA phenylthiazole **1** has two

essential structural features: a lipophilic tail and a cationic aminoguanidinyl head (Figure 1).[18] Considering these two fundamental structural elements, an in-house library of nearly three-hundred compounds, all with the guanidine or aminoguanidine functional group on one end and a less lipophilic chain at the opposite end, was screened using whole-cell screening assay. The antibacterial activity of the top promising structures in the preliminary screening, which successfully passed the PAINS assay,[22] were selected and their antibacterial activity was further assessed against a clinical isolate of MRSA NRS123. These efforts, collectively, furnished compounds in Figure 2 as lead structures.

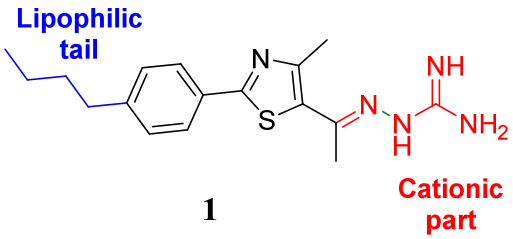

1

Figure 1. Chemical structure of first hit compound.

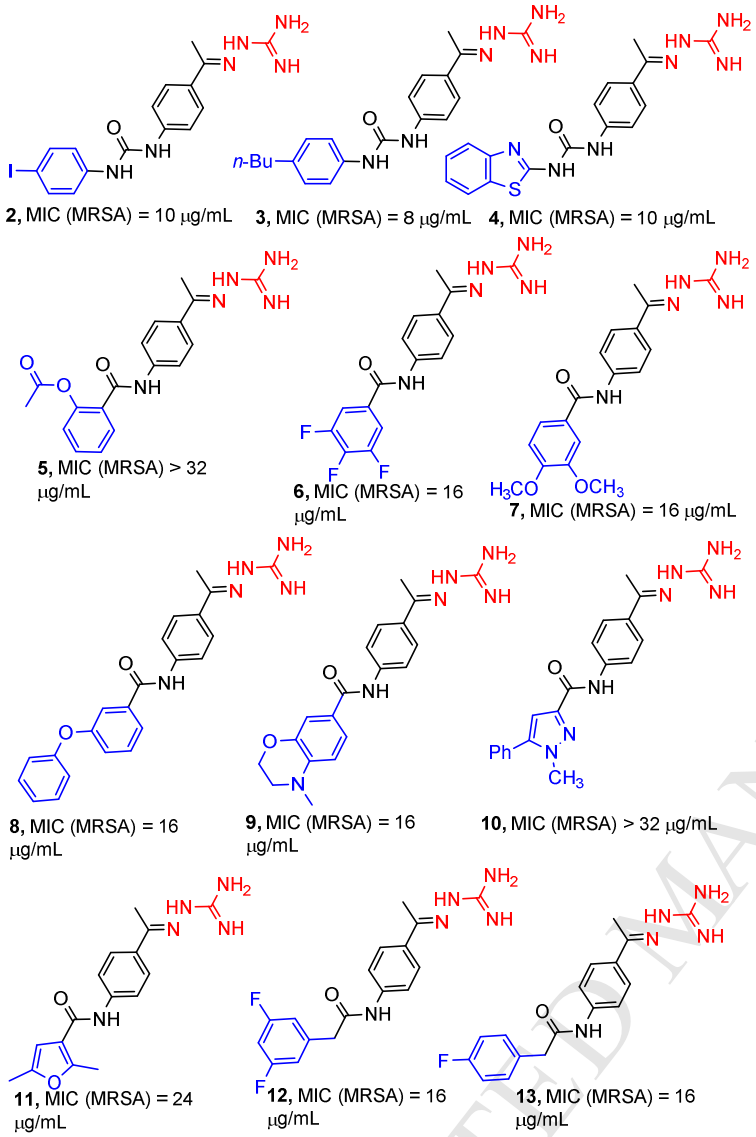

Figure 2. Chemical structures of new hits with their minimum inhibitory concentration (MIC) values against MRSA NRS123, All compounds were checked for pan-assay interference compounds (PAINS) and none are PAINS.[22]

According to the chemical nature of the linker, the active hits can be classified into diarylurea derivatives (compounds **2**-**4**), *N*-phenylarylamide analogues (compounds **5**-**9**) and *N*-phenylacetamides (compounds **12** and **13**). The highest anti-MRSA activity was observed with the diarylurea compounds **2**-**4**. Additionally, after exploring the literature, we have found some reports that address the antimicrobial activity of diphenylurea derivatives,[23] in addition to many others as antitumor.[24] Therefore, chemical modifications reported here involved building a

focused library of diphenylureas with different lipophilic moieties at the phenyl *para* position to define the structure−activity relationships (SARs) at this position in a rigorous manner.

Taking the metabolic stability and other key pharmacokinetic properties into account to finally develop a drug-candidate, this work has three objectives: to investigate the antimicrobial activity of the diphenylureas against a panel of MRSA and VRSA clinical isolates, to investigate the capability of the most promising candidate to penetrate and eradicate intracellular MRSA, and to confirm the potent anti-MRSA activity of the most promising analogue in a *Caenorhabditis elegans* animal model.

2. RESULTS AND DISCUSSION

2.1. CHEMISTRY**.** The diphenylurea **16** was obtained by allowing *t*-butylaniline to react with the isocyanate **15**. Treatment of the obtained acetyldiphenylurea **16** with aminoguanidine, in the presence of lithium chloride as a catalyst, afforded the final product **17** (Scheme 1). Similarly, the 1-(4-acetylphenyl)-3-(4-hydroxyphenyl)urea (**19**) was prepared (Scheme 2). The latter compound was allowed to react with a series of alkyl bromides to give the alkylated products **20a-o**. These products were then treated with aminoguanidine to afford the final products **21a-o** (Scheme 2).

Scheme 1.

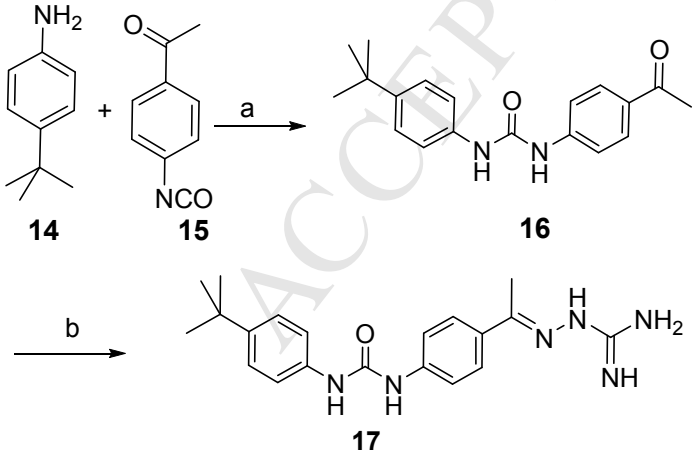

Reagents and conditions: a) dry THF, 78 ^{o}C; b) aminoguanidine HCl, EtOH, 78 ^{o}C

Scheme 2.

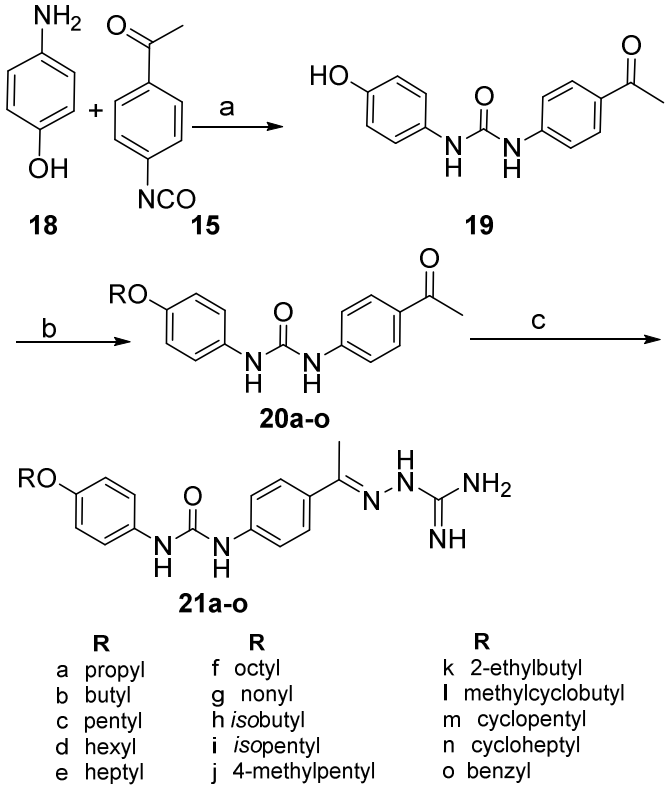

R	R	R
a propyl	f octyl	k 2-ethylbutyl
b butyl	g nonyl	l methylcyclobutyl
c pentyl	h *iso*butyl	m cyclopentyl
d hexyl	i *iso*pentyl	n cycloheptyl
e heptyl	j 4-methylpentyl	o benzyl

Reagents and conditions: a) dry THF, 78 °C; b) RX, DMF, K_2CO_3; c) aminoguanidine HCl, EtOH, 78 °C

2.2. BIOLOGICAL RESULTS AND DISCUSSION.

Among all tested hits, the three disubstituted urea derivatives **2-4** showed the best antibacterial effect with minimum inhibitory concentration (MIC) values ranging between 8 and 10 µg/mL. Compound **3** was chosen for further analysis and its stability to hepatic metabolism was briefly studied. Surprisingly, compound **3** was found to be a good substrate for the CYP450 enzymes resulting in an ultra-short half-life ($t_{1/2}$) of 13.0 minutes and high clearance rate when incubated with human liver microsomes (HLM) (Table 2). Microsomal oxidation of **3** might occur at multiple positions; for instance, aromatic and benzylic oxidation are highly expected. Since the active site of CYP450 is surrounded by a highly hydrophobic seven phenylalanine cluster,[25] the benzylic carbon of **3** was initially posited to be the metabolic soft-spot (Figure 3). This particular carbon is hypothesized to be extensively oxidized by metabolic enzymes. Gratifyingly, literature is full of solutions for rapidly metabolized benzylic carbons that include adding

two methyl groups or substitution with an oxygen atom.[26, 27] Therefore, two derivatives possessing a side chain with the same number of carbon atoms were prepared; one with *t*-butyl (compound **17**), and one with a butoxy moiety (compound **21b**). The *t*-butyl analogue **17** showed negligible anti-MRSA activity, while the antibacterial effect of **21b** was reasonable with MIC values ranging between 8 and 16 µg/mL (Table 1). Even more interesting, compounds **17** and **21b** exhibit a marked improvement in their stability to hepatic metabolism as noted by their increased half-lives and lower clearance rates (Table 2). Briefly, compound **21b** showed a $t_{1/2}$ that was five times longer and a lower microsomal clearance rate than the corresponding butyl hit compound **3** (Table 2). Additionally, **21b** exhibited a longer half-life than two commercially-available drugs, midazolam ($t_{1/2}$ = 5.7 minutes) and verapamil ($t_{1/2}$ = 15.3 minutes). The longer half-life values of **17** and **21b** support our hypothesis of the presence of metabolic soft spot at the pended *n*-butyl moiety. However, this information must be taken with caution as it doesn't completely exclude the possibility of aromatic hydroxylation. What can be concluded from the MIC and metabolic stability analyses of compounds **17** and **21b** is that diphenylureas containing an alkoxy side chain represent a promising novel scaffold, with suitable drug-like properties, to construct a novel class of antimicrobial agents. Additionally, the accessibility of the synthetic protocol for ether formation and the availability of a variety of commercial alkyl halides permit a complete study of the structure-activity and structure-kinetics relationships at this particular position.

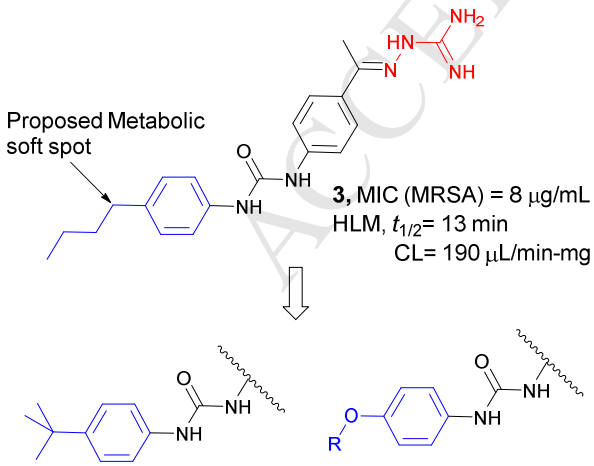

Figure 3. Proposed metabolic soft spot and strategies to decrease affinity to CYP450.

Next, a series of alkoxy side chains was tethered with the core of the diphenylurea in order to rigorously address the structure-activity and structure-kinetics relationships at this position. Thus far, fifteen derivatives with different homologous, branched and cyclic side chains have been synthesized and tested against a panel of methicillin-sensitive *S. aureus* (MSSA), MRSA and VRSA clinical isolates. Compounds **21c**, **21d**, **21h**, **21i**, **21j** and **21n** are the most potent compounds against *S. aureus* with MIC values in the range of 2 to 8 µg/mL (Table 1). They appear to be bactericidal given the minimum bactericidal concentration (MBC) values match or are one-fold higher than the MIC values against most clinical isolates. Interestingly, the newly developed diphenylureas maintained their potent antibacterial effect when tested against strains exhibiting high-level resistance to vancomycin (VRSA4 and VRSA10). In this regard, they have an advantage over vancomycin.

From SAR point of view, increasing the number of methylene units from 4 (as in the lead compound **21b**) to five or six (compounds **21c** and **21d**) remarkably ameliorates the antibacterial activity of these compounds (Table 1). The branched analogue **21i** with a six carbon-unit side chain demonstrated MIC values on par with that of linezolid, an agent of last resort for treatment of systemic MRSA infections. Unlike the bacteriostatic nature of linezolid,[28] compound **21i** appears to be bactericidal, given its MBC value matches or is one-fold higher than its MIC value against all strains of *S. aureus* tested.

Table 1. The minimum inhibitory concentration (MIC in µg/mL) and the minimum bactericidal concentration (MBC µg/mL) of diphenylurea compounds screened against *S. aureus* isolates.

	***S. aureus* NRS107 (RN4220)**		**MRSA NRS123 (USA400)**		**MRSA NRS382 (USA100)**		**MRSA NRS383 (USA200)**		**MRSA NRS384 (USA300)**		**VRSA4**		**VRSA10**	
	MIC	**MBC**	**MIC**	**MBC**	**MIC**	**MBC**	**MIC**	**MBC**	**MIC**	**MBC**	**MIC**	**MBC**	**MIC**	**MBC**
17	-	-	-	-	64	128	-	-	-	-	-	-	-	-
21a	8	8	4	16	8	8	8	16	8	16	8	8	8	16
21b	16	>64	8	32	16	16	16	32	16	16	16	16	16	32
21c	4	8	4	16	4	4	4	4	4	4	4	4	4	8
21d	8	8	8	16	4	4	4	8	8	16	8	8	8	8
21e	8	8	16	16	16	16	8	8	16	16	8	8	16	16
21f	16	32	32	32	16	32	16	16	16	16	16	32	16	32
21g	32	64	32	64	32	32	16	32	32	32	16	16	32	32
21h	4	4	8	16	8	8	4	4	4	8	4	8	4	8
21i	2	4	2	4	4	4	2	4	2	4	4	4	2	4

	S. aureus NRS107 (RN4220)		MRSA NRS123 (USA400)		MRSA NRS382 (USA100)		MRSA NRS383 (USA200)		MRSA NRS384 (USA300)		VRSA4		VRSA10	
	MIC	**MBC**	**MIC**	**MBC**	**MIC**	**MBC**	**MIC**	**MBC**	**MIC**	**MBC**	**MIC**	**MBC**	**MIC**	**MBC**
21j	4	4	4	8	4	8	4	8	8	8	4	4	4	4
21k	-	-	-	-	128	-	-	-	-	-	-	-	-	-
21l	16	16	16	32	16	16	16	32	16	16	16	16	16	32
21m	-	-	-	-	64	64	64	128	-	-	-	-	-	-
21n	2	4	4	4	2	4	2	4	2	4	2	4	8	8
21o	8	8	8	>64	4	>128	8	16	8	8	8	8	8	>64
Linezolid	2	32	2	32	2	16	2	32	2	16	2	8	2	16
Vanco-mycin	1	1	0.5	0.5	<1	<1	0.5	0.5	0.5	1	>128	>128	>128	>128

Table 2. Metabolic stability analysis of compounds **3**, **17**, **21b**, and **21n** in human liver microsomes.

Tested compound	NADPH-Dependent CL_{int} (µL/min-mg)	NADPH-Dependent $T_{1/2}$ (min)	NADPH-Free CL_{int} (µl/min-mg)	NADPH-Free $T_{1/2}$ (min)	Notes
Midazolam	402	5.7	< 9.6	>240	High clearance control
Verapamil	151	15.3	< 9.6	>240	High clearance control
Warfarin	< 9.6	> 240	< 9.6	>240	Low clearance control
3	189.8	13.0	ND	ND	
17	20.0	174	ND	ND	
21b	51.0	65.5	ND	ND	
21n	33.9	68.2	42.9	53.8	

The two cornerstone antimicrobials clinically in use for the treatment of systemic MRSA infections are glycopeptides such as vancomycin and oxazolidinones such as linezolid. Each of these categories has its own drawbacks that affect their clinical efficiency. While linezolid is a bacteriostatic agent,[28] vancomycin exhibits a very slow bactericidal mode of action[29] resulting in difficulty in clearing an infection[30] and clinical failure in many cases.[31] In order to further investigate the observed bactericidal activity of the new diphenylurea derivatives, the most promising compounds **21i**, **21j**, and **21n** (at 4 × MIC) were further examined against MRSA USA400 using a standard time-kill assay. All three compounds were able to eradicate a high inoculum of MRSA within four hours. This confirms they possess rapid bactericidal activity. Vancomycin requires 24 hours to achieve the same effect (Figure 4). The rapid bactericidal activity of the diphenylurea compounds may limit the ability of MRSA to rapidly

acquire resistance to these agents. Indeed, repeated subculturing of MRSA to the diphenylurea compounds over a two-week period did not result in the isolation of resistant mutants via a multi-step resistance assay (data not shown).

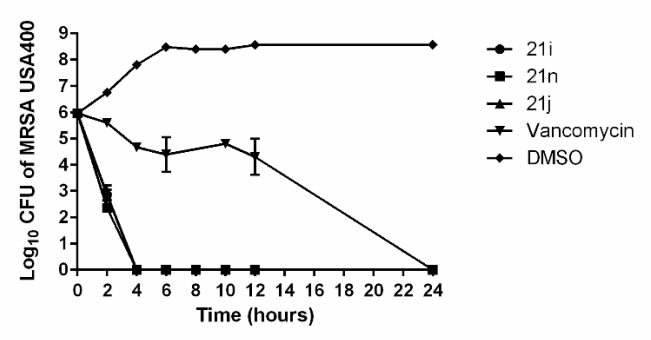

Figure 4. Time-kill analysis of diphenylurea compounds 21i, 21n, 21j, and vancomycin against methicillin-resistant *Staphylococcus aureus* (MRSA USA400) over a 24-hour incubation period at 37 °C. DMSO served as a negative control. The error bars represent standard deviation values obtained from triplicate samples used for each compound/antibiotic studied.

Thus far, our analysis of the antibacterial activity of the diphenylurea compounds focused exclusively on their effect on extracellular MRSA. However, MRSA is not exclusively an extracellular pathogen. Rather, MRSA can escape and hide intracellularly within immune cells, such as macrophages[32, 33] inducing several life-threating diseases such as pneumonia in humans[34] and mastitis in cattle. MRSA harbouring inside host tissues can lead to recurring infections that are very challenging for clinicians to treat.[35] This poses a unique challenge as many antibiotics are unable to enter inside infected cells to eradicate MRSA. For instance, the inability of vancomycin, and other glycopeptides, to penetrate and sufficiently accumulate inside macrophages[34] has led to clinical failure in more than 40% of cases treated with a standard vancomycin dosing regimen.[36]

Prior to examining the ability of our diphenylureas to penetrate and kill intracellular MRSA, the most active compounds were subjected to a preliminary toxicity profiling using human keratinocytes (HaCaT). Figure 5 indicates that the most tolerable compounds were **21c**, **21n** and **21i** as they were not toxic up to a concentration of 64 μg/mL (or 32 μg/mL for **21i**). This represents an 8-to 16-fold difference between the

MIC values obtained against MRSA for all three compounds. Compounds **21c** and **21i** are structurally analogous; thus **21n** and **21i** were selected for further investigation to examine their ability to kill intracellular MRSA harbouring inside infected macrophages.

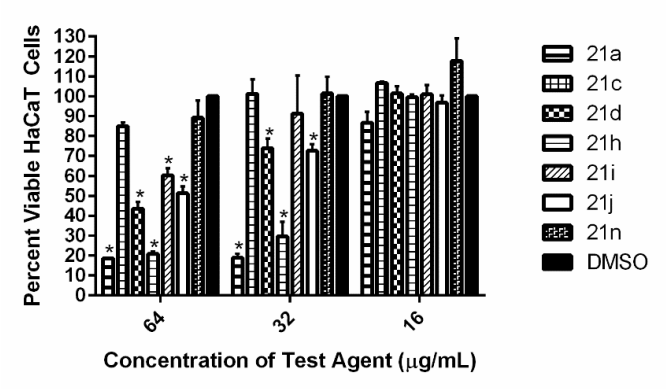

Figure 5. Toxicity analysis of diphenylurea compounds against human keratinocytes (HaCaT). Percent viable mammalian cells (measured as average absorbance ratio (test agent relative to DMSO)) for cytotoxicity analysis of diphenylurea compounds **21d, 21h, 21c, 21i, 21a, 21n**, and **21j** (tested in triplicate) at 16, 32, and 64 μg/mL against HaCaT cells using the MTS 3-(4,5-dimethylthiazol-2-yl)-5-(3-carboxymethoxyphenyl)-2-(4-sulfophenyl)-2*H*-tetrazolium) assay. Dimethyl sulfoxide (DMSO) was used as a negative control to determine a baseline measurement for the cytotoxic impact of each compound. The absorbance values represent an average of a minimum of three samples analyzed for each compound. Error bars represent standard deviation values for the absorbance values. A one-way ANOVA, with post hoc Dunnet's multiple comparisons test, determined statistical difference between the values obtained for each compound and DMSO (denoted by the asterisk) ($P < 0.05$).

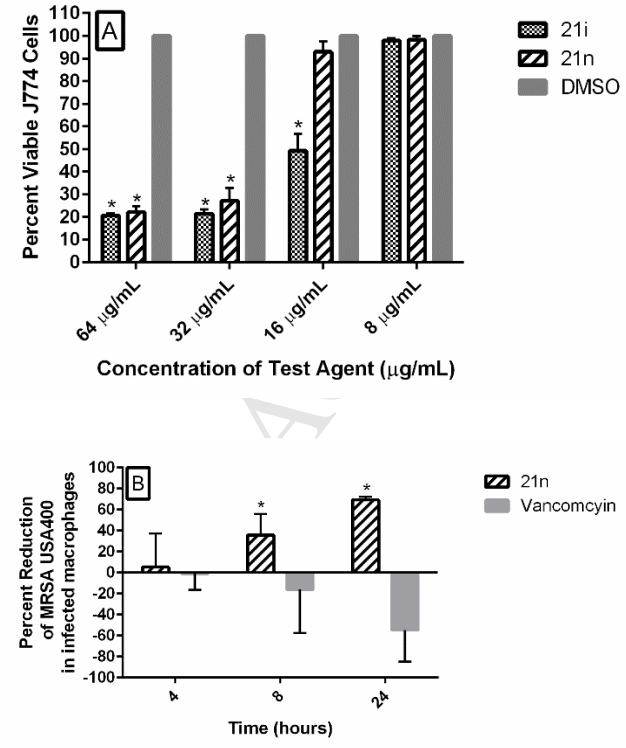

Figure 6. Toxicity analysis and examination of clearance of intracellular MRSA present in murine macrophage (J774) cells. Panel A) Percent viable mammalian cells (measured as average absorbance ratio (test agent relative to DMSO)) for cytotoxicity analysis of diphenylurea compounds **21i** and **21n** (tested in triplicate) at 8, 16, 32, and 64 µg/mL against J774 cells using the MTS 3-(4,5-dimethylthiazol-2-yl)-5-(3-carboxymethoxyphenyl)-2-(4-sulfophenyl)-2*H*-tetrazolium) assay. Dimethyl sulfoxide (DMSO) was used as a negative control to determine a baseline measurement for the cytotoxic impact of each compound. The absorbance values represent an average of a minimum of three samples analyzed for each compound. Error bars represent standard deviation values for the absorbance values. A one-way ANOVA, with post hoc Dunnet's multiple comparisons test, determined statistical difference between the values obtained for each compound and DMSO (denoted by the asterisk) ($P < 0.05$). **Panel B)** Percent reduction of MRSA USA400 colony forming units inside infected murine macrophage cells after treatment with 16 µg/mL of either compound **21n** or vancomycin (tested in triplicate) for 4, 8, and 24 hours. Data were analyzed via a Student's t-test ($P < 0.05$). Asterisks (*) represent significant difference between treatment of J774 cells with **21n** in comparison to vancomycin.

Initial J774 cell tolerability screening of **21i** and **21n** revealed that compound **21n** is not toxic up to 16 µg/mL; however, compound **21i** appears toxic to J774 cells even at a concentration as low as 8 µg/mL (Figure 6A). Due to its superior toxicity profile, compound **21n** was selected for further analysis for its ability to clear MRSA harboring inside macrophage cells. As depicted in Figure 6B, after four hours, **21n** (same time required to eradicate extracellular MRSA completely via a time-kill assay) produced a 5% reduction in MRSA CFU/mL when compared to untreated samples. The number steadily increased and reached 35.7% reduction of MRSA after 8 hours and 69% reduction after 24 hours of treatment. Vancomycin, as expected, was not able to reduce the presence of MRSA inside infected J774 cells, even after 24 hours of treatment. The results collectively indicate compound **21n** has the ability to gain entry into macrophage cells (after 8 hours of treatment) at a concentration high enough to significantly reduce the burden of MRSA inside infected macrophage cells.

After confirming this newly discovered class of compounds has potent antibacterial activity against extracellular and intracellular MRSA with a well-tolerated safety profile against mammalian cells, we moved to ensure that the mechanism of action of these compounds was not through physical disruption of the bacterial cell membrane. Membrane-active agents are typically non-specific (i.e. can disrupt both bacterial and eukaryotic cells) and thus have limited utility as therapeutic agents.

To examine if the diphenylurea compounds exert their antibacterial effect by targeted disruption of the bacterial cell membrane, compounds **21i**, **21n**, and vancomycin were incubated at a high concentration (5.0 × MIC value) with a high-inoculum of MRSA NRS123 (USA400). Lysostaphin, a well-characterized membrane-disruptive agent against *S. aureus*, was used as a positive control. The mechanism of action of compounds **21i** and **21n** does not appear to be through physical disruption of the integrity of the bacterial cell membrane (Figure 7). The compounds mimic the behavior of vancomycin, an antibiotic that inhibits bacterial cell wall synthesis, and untreated samples (<15% leakage of 260 and 280 nm absorbing material observed) in contrast to cells treated with lysostaphin. Subsequent investigation into the mechanism of action of the diphenylureas indicates they interfere with bacterial cell wall synthesis (data not published). At present, we are working to validate these findings.

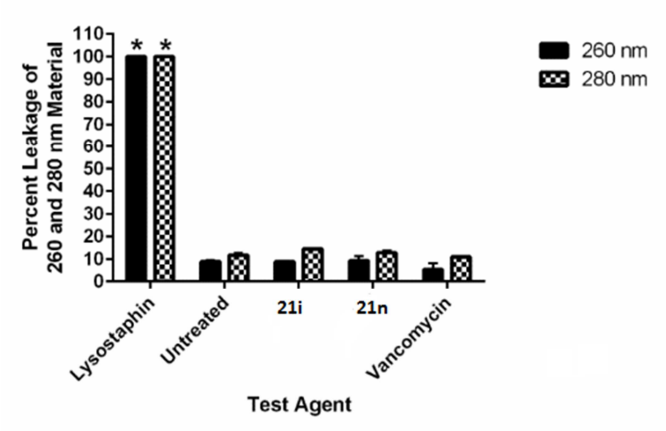

Figure 7. Loss of 260 and 280 nm cellular absorbing material for compounds 21i and 21n against MRSA NRS123. Untreated cells represent the negative control while 20 µg/mL lysostaphin (in 50 mM Tris-HCl, pH 7.6) served as the positive control. The figure represents the ratio of the average absorbance value obtained for each treatment against the average absorbance value obtained for the positive control. The error bars represent standard deviation values of duplicate samples for each treatment option. A paired t-test, $P \leq 0.05$, demonstrated no statistical difference between the values obtained for vancomycin and compounds **21i** and **21n** relative to untreated cells but significant difference (denoted by *) in the absorbance values obtained for lysostaphin as compared to untreated cells.

***In vivo* examination of 21n and vancomycin to kill MRSA USA400 in a *Caenorhabditis elegans* animal model**. Thus far, promising *in vitro* results pertaining to the anti-MRSA activity of the diphenylurea compounds was obtained. However, it is critical to validate *in vitro* results *in vivo*, in a

suitable animal model of infection. To examine the efficacy of the diphenylurea compounds to treat a MRSA infection *in vivo*, the *Caenorhabditis elegans* (*C. elegans*) was utilized. The *C. elegans* animal model is an established system for investigating the efficacy of small molecule antibacterial agents *in vivo* in early stage drug discovery[37, 38] Using this model, compound **21n** (at 10 µg/mL, equal to 2.5 × MIC) retains its potent antibacterial activity *in vivo* reducing the burden of MRSA USA400 by more than 50% in infected worms (Figure 8). Vancomycin, at the same concentration, reduces the bacterial burden by 25%.

Compound **21n** thus far emerged as the most promising candidate for further investigation. In order to gauge potential therapeutic applications for **21n**, it was critical to examine its pharmacokinetic profile first. This information will prove valuable in designing future animal studies involving MRSA infections (systemic and localized) including identifying an appropriate route of administration and frequency of dosing.

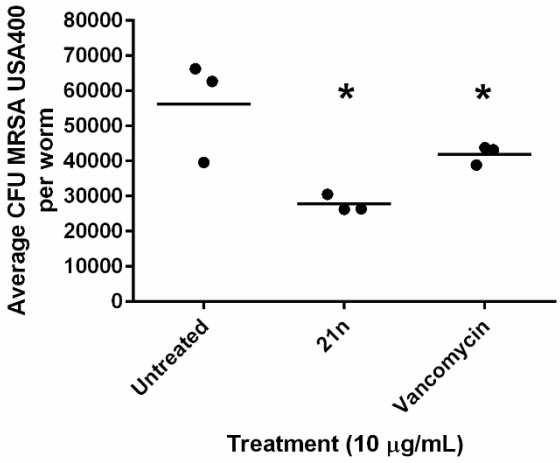

Figure 8. Antibacterial activity of 21n and vancomycin *in vivo* against MRSA-infected *C. elegans*. *In vivo* examination of antibacterial activity of diphenylurea compound **21n** and vancomycin (tested at 10 µg/mL) in *C. elegans* AU37 infected with methicillin-resistant *Staphylococcus aureus* USA400. Vancomycin served as a positive control. Worms (in L4 stage of growth) were infected with bacteria for six hours before transferring 15-25 worms to wells of a 96-well plate. Test agents were added and incubated with worms for 20 hours. Worms were sacrificed and the number of viable colony-forming units of MRSA USA400 in infected worms was determined for each treatment regimen. The figure presents the average CFU/mL of MRSA USA400 for each treatment condition. Asterisk (*) denotes statistical significance ($P < 0.05$) in CFU/mL relative to untreated control using a Student's t-test (with Holm-Sidak correction).

Pharmacokinetic profiling

Permeability assay. We initially investigated the ability of compound **21n** to permeate across the gastrointestinal tract as modeled by the Caco-2 bidirectional permeability assay. Compound **21n** is able to permeate across the Caco-2 membrane (from the apical to basolateral direction) however at a slow rate that is similar to talinolol (Table 3). The high efflux ratio for **21n** indicates the permeability of this compound is significantly impaired by the presence of the P-glycoprotein efflux transport system (P-gp). This result would indicate that, for systemic application, **21n** would be more suitable for administration intravenously. As an alternative to systemic application, the compound could also be explored for topical treatment of MRSA skin lesions. Given *S. aureus* is responsible for more than half of all skin and soft tissue infections in the United States,[39] topical antibiotics are valuable allies to treat these particular infections. This point will be further explored with **21n** in a future study.

Metabolic stability analysis. As discussed earlier, the lead diphenylurea **3** that carries a *n*-butyl moiety at the lipophilic side chain revealed an ultra-short half-life ($t_{1/2}$ = 13 min) with a clearance rate close to 190 μL/min-mg (Table 2). Such PK data (rapid clearance and short $t_{1/2}$) will significantly affect the size and frequency of the dosing regimen. Therefore, following well-established protocols,[26, 27] the benzylic metabolic soft spot was replaced with an oxygen atom, which cannot be oxidized under physiological conditions. The alkoxy analogues synthesized exhibited a noticeably higher half-life value (five-fold greater than compound **3**) and lower clearance rates (3-5 times lower than for compound **3**) (Table 2).

In particular, compound **21n** is superior to both midazolam and verapamil as it is cleared by human liver microsomes at a much lower rate than both control drugs (Table 2). The half-life of 68.2 minutes indicates the compound is metabolized at a moderate rate. Interestingly, the clearance rate increases and the half-life decreases for compound **21n** in the absence of NADPH indicating this compound is not metabolized via the typical cytochrome-P450 system in the liver.

Table 3. Caco-2 bidirectional permeability analysis for compound **21n**.

Test Article	Test Concentration (μM)	Assay Duration (hours)	Mean A→B P_{app} (10^{-6} cm/sec)	Mean B→A P_{app} (10^{-6} cm/sec)	Efflux ratio (R_e)	Notes
Ranitidine	10	2	0.235	2.31	9.8	Low permeability control
Talinolol	10	2	0.065	8.95	138	P-glycoprotein efflux transporter control
Warfarin	10	2	27.7	20.3	0.73	High permeability control
21n	10	2	0.039	51.9	>1000	

***In vivo* Pharmacokinetics**. Caco-2 results tend to over predict efflux due to P-gp overexpression. Thus, an *in vivo* PK assessment was conducted. Briefly, a dose of 50 mg/kg was given to male Sprague−Dawley rats and blood samples were collected over a 24-hour period. The aim of this preliminary assessment was to identify the most suitable route of administration for examining the efficacy of **21n** in more advanced animal models of MRSA infection.

Thus far, the *in vivo* PK results confirmed the high affinity of **21n** to P-gp as the maximum detected plasma concentration (C_{max}) for **21n** was around 16 ng/mL (Table 4). This value is roughly two-hundred times less than the average MIC value of **21n** against MRSA. Apart from the high affinity to P-gp, the high duration of action, indicated by the half-life ($t_{1/2}$) value of approximately 16 hours (Table 4) further supports our hypothesis that the benzylic methylene unit is the metabolic soft spot. Thus presently, **21n** would be more suitable to be examined for efficacy in suitable mouse models of infection either through intravenous administration (for systemic MRSA infections) or topically (for MRSA skin infections).

Table 4. Oral pharmacokinetic parameters in rats after 50 mg/kg oral dose of compound **21n**.

Animal	C_{max} (ng/mL)	T_{max} (h)	AUC_{last} ((h)*(ng/mL))	AUC_{tot} ((h)*(ng/mL))	Lz (1/h)	t_{half} (h)	MRT (h)
1	17.300	8.000	207.203	405.515	0.039	17.714	30.467
2	8.640	12.000	137.315	286.033	0.037	18.641	32.875
3	22.900	8.000	310.805	461.493	0.060	11.593	21.828
N	3	3	3	3	3	3	3
Mean	16.280	9.333	218.441	384.347	0.045	15.982	28.390
Stdev	7.185	2.309	87.289	89.625	0.013	3.830	5.809

%CV	44.131	24.744	39.960	23.319	27.615	23.963	20.461
SEM	4.148	1.333	50.396	51.745	0.007	2.211	3.354
Min	8.640	8.000	137.315	286.033	0.037	11.593	21.828
Median	17.300	8.000	207.203	405.515	0.039	17.714	30.467
Max	22.900	12.000	310.805	461.493	0.060	18.641	32.875

3. CONCLUSION.

Bacterial resistance to currently available antibiotics represents a significant challenge to healthcare providers and researchers in drug discovery. New antibacterial agents with unique chemical scaffolds and mechanism of action are urgently needed. The present study reported a new series of synthetic compounds bearing the diphenylurea scaffold with potent antibacterial activity against MRSA and VRSA. Compound **21n** emerged as the most promising analogue due to its superior toxicity profile, ability to kill intracellular MRSA harboring inside infected macrophages, enhanced stability to hepatic metabolism, and potent anti-MRSA activity *in vivo* in a *C. elegans* model. Pharmacokinetic analysis of **21n** revealed, at present, it is suitable for administration intravenously or topically (for treatment MRSA skin infections). Future studies will aim to examine **21n** in suitable mouse models of MRSA infection and to develop novel analogues with enhanced ability to permeate across the gastrointestinal tract (to permit oral dosing).

4. EXPERIMENTAL SECTION

4.1.CHEMISTRY

4.1.1. General. ^{1}H NMR spectra were run at 300 MHz and ^{13}C spectra were determined at 100 MHz in deuterated chloroform ($CDCl_3$), or dimethyl sulfoxide (DMSO-d_6) on a Varian Mercury VX-400 NMR spectrometer. Chemical shifts are given in parts per million (ppm) on the delta (δ) scale. Chemical shifts were calibrated relative to those of the solvents. Flash chromatography was performed on 230-400 mesh silica. The progress of reactions was monitored with Merck silica gel IB2-F plates (0.25 mm thickness). The infrared spectra were recorded in potassium bromide disks on pye Unicam SP 3300 and Shimadzu FT IR 8101 PC infrared spectrophotometer. Mass spectra were recorded at 70 eV. High resolution mass spectra for all ionization techniques were obtained from a FinniganMAT XL95. Melting points were

determined using capillary tubes with a Stuart SMP30 apparatus and are uncorrected. HPLC analyses were performed on an Agilent binary HPLC system (Model 1260) equipped with a multiple wavelength absorbance UV detector set for 254 nM, and using a 5 μM C-18 reversed-phase column and methanol:water (4:1) as a mobile phase. All yields reported refer to isolated yields

4.1.2. Preparation of Diphenylurea Derivatives 16 and 19. General Procedure. An appropriate amine (1 equiv.) was added to 4-acetylphenyl isocyante (**15**, 1 equiv.) in dry THF (20 mL). The reaction mixture was stirred at room temperature for 12 hours. The solvent was evaporated under reduced pressure. The crude product was purified by crystallization from methanol-ethyl acetate (1:1) to afford the desired compounds.

4.1.2.1. 1-(4-Acetylphenyl)-3-(4-*tert*-butylphenyl)urea (16).[40] Grayish-white solid (58% yield). ^{1}H NMR (DMSO-d_6) δ 9.14 (brs, 1 H), 8.79 (brs, 1 H), 7.88 (d, J = 8.7 Hz, 2 H), 7.61 (d, J = 8.7 Hz, 2 H), 7.41 (d, J = 8.7 Hz, 2 H), 7.13 (d, J = 8.7 Hz, 2 H), 2.56 (s, 3 H), 1.25 (s, 9 H); ESIMS *m/z* (rel intensity) 310 (M^+, 100); HRMS (ESI), *m/z* 310.1677 M^+, calcd for $C_{19}H_{22}N_2O_2$ 310.1781.

4.1.2.2. 1-(4-acetylphenyl)-3-(4-hydroxyphenyl)urea (19).[40] Off-white solid (80% yield). R_f 0.36 (50% EtOAc/hexanes); ^{1}H NMR (DMSO-d_6, 300 MHz) δ 9.11(s, 1H), 8.97 (s, 1H), 8.46 (s, 1H), 7.90 (d, J = 11.70 Hz, 2H), 7.57 (d, J = 11.70, 2H), 7.24 (d, J = 11.40, 2H), 6.71 (d, J = 11.07, 2H), 2.49 (s, 3H); HRMS *m/z* 270.1015 (calcd for $C_{15}H_{14}N_2O_3$, 270.1004); Anal. Calcd for $C_{15}H_{14}N_2O_3$: C, 66.66; H, 5.22; N, 10.36; found: C, 66.94; H, 5.28; N, 10.59.

4.1.3. General procedure for the nucleophilic substitution reaction. A solution of urea derivative **19** (0.17 g, 0.5 mmol), alkylhalide (1.0 mmol, 2 eq) and K_2CO_3 in DMF (5 mL) was stirred at 100 °C for 12 hours. After completion as indicated by TLC, 5.0 mL of EtOAc was added and the mixture was poured into a saturated solution of $NaHCO_3$ (15 mL). The heterogeneous mixture was separated and the aqueous layer was extracted with EtOAc (3 × 10 mL). The combined organic layers were washed with brine, dried

over $MgSO_4$, filtered through celite and concentrated under reduced pressure. Purification by flash chromatography on silica gel using EtOAc-hexanes for elution provided the title compounds.

4.1.3.1. 1-(4-acetylphenyl)-3-(4-propoxyphenyl)urea (20a).[40] Off-white solid (70% yield, 95 mg). R_f 0.75 (50% EtOAc/hexanes); ^{1}H NMR (DMSO-d_6, 300MHz) δ 8.99 (s, 1H), 8.57 (s, 1H), 7.90 (d, *J* = 9.00, 2H), 7.58 (d, *J* = 8.70, 2H), 7.36 (d, *J* = 9.30 Hz, 2H), 6.88 (d, *J* = 9.30 Hz, 2H), 3.90 (t, *J* = 6.60 Hz, 2H) 2.49 (s, 3H), 1.74–1.67 (m, 2H), 0.99 (t, *J* = 7.50, 3H); ^{13}C NMR (DMSO-d_6) δ 196.18, 154.14, 152.27, 144.52, 132.10, 130.21, 129.57, 120.28, 116.96, 114.60, 69.09, 26.27, 22.04, 10.35; HRMS *m/z* 312.1466 (calcd for $C_{18}H_{20}N_2O_3$, 312.1474); Anal. Calcd for $C_{18}H_{20}N_2O_3$ (312.14): C, 69.21; H, 6.45; N, 8.97; found: C, 69.47; H, 6.51; N, 9.02.

4.1.3.2. 1-(4-Acetylphenyl)-3-(4-butoxyphenyl)urea (20b). Off-white solid (82% yield, 133 mg). R_f 0.77 (50% EtOAc/hexanes); ^{1}H NMR (DMSO-d_6, 300MHz) δ 8.99 (s, 1H), 8.57 (s, 1H),7.90 (d, *J* = 8.70, 2H), 7.58 (d, *J* = 8.70, 2H), 7.36 (d, *J* = 9.00, 2H), 6.88 (d, *J* = 9.00, 2H), 3.94 (t, *J* = 6.60, 2H) 2.49(s, 3H), 1.74–1.67 (m, 2H), 1.47–1.41 (m, 2H), 0.99 (t, *J* = 7.20, 3H); HRMS *m/z* 326.1635 (calcd for $C_{19}H_{22}N_2O_3$, 326.1630); Anal. Calcd for $C_{19}H_{22}N_2O_3$ (326.16): C, 69.92; H, 6.79; N, 8.58; found: C, 70.21; H, 6.87; N, 8.84.

4.1.3.3. 1-(4-acetylphenyl)-3-(4-(pentyloxy)phenyl)urea (20c). Off-white solid (65% yield, 104 mg). R_f 0.79 (50% EtOAc/hexanes); ^{1}H NMR (DMSO-d_6, 300MHz) δ9.01 (s, 1H), 8.59 (s, 1H),7.90 (d, *J* = 8.70, 2H), 7.58 (d, *J* = 8.40, 2H), 7.36 (d, *J* = 9.00, 2H), 6.88 (d, *J* = 9.00, 2H), 3.94 (t, *J* = 6.60, 2H), 2.49 (s, 3H), 1.71–1.65 (m, 2H), 1.37–1.31 (m, 4H), 0.92–0.84 (m, 3H); HRMS *m/z* 340.1790 (calcd for $C_{20}H_{24}N_2O_3$, 340.1787); Anal. Calcd for $C_{20}H_{24}N_2O_3$ (340.17): C, 70.57; H, 7.11; N, 8.23; found: C, 70.74; H, 7.18; N, 8.31.

4.1.3.4. 1-(4-acetylphenyl)-3-(4-(hexyloxy)phenyl)urea (20d). Off-white solid (80% yield, 71 mg). R_f 0.81 (50% EtOAc/hexanes); ^{1}H NMR (DMSO-d_6, 300MHz) δ 9.04 (s, 1H), 8.62 (s, 1H),7.90 (d, *J* = 8.70, 2H), 7.58 (d, *J* = 8.40, 2H), 7.36 (d, *J* = 8.10, 2H), 6.88 (d, *J* = 8.70, 2H), 3.93 (t, *J* = 6.30, 2H), 2.49 (s, 3H), 1.70–1.64 (m, 2H), 1.40–1.29 (m, 6H), 0.87–0.85 (m, 3H); HRMS *m/z* 354.1930 (calcd for

$C_{21}H_{26}N_2O_3$, 354.1943); Anal. Calcd for $C_{21}H_{26}N_2O_3$ (354.19): C, 71.16; H, 7.39; N, 7.90; found: C, 71.38; H, 7.46; N, 8.02.

4.1.3.5. 1-(4-Acetylphenyl)-3-(4-(heptyloxy)phenyl)urea (20e). Off-white solid (84% yield, 154 mg). R_f 0.8 (50% EtOAc/hexanes); ^{1}H NMR (DMSO-d_6, 300MHz) δ 8.99 (s, 1H), 8.57 (s, 1H),7.90 (d, *J* = 8.70, 2H), 7.58 (d, *J* = 8.70, 2H), 7.36 (d, *J* = 9.00, 2H), 6.88 (d, *J* = 9.30, 2H), 3.93 (t, *J* = 6.60, 2H), 2.49 (s, 3H), 1.71–1.66 (m, 2H), 1.42–1.28 (m, 8H), 0.89–0.85 (m, 3H); HRMS 368.2107 (calcd for $C_{22}H_{28}N_2O_3$, 368.2100); Anal. Calcd for $C_{22}H_{28}N_2O_3$ (368.21): C, 71.71; H, 7.66; N, 7.60; found: C, 71.88; H, 7.72; N, 7.84.

4.1.3.6. 1-(4-Acetylphenyl)-3-(4-(octyloxy)phenyl)urea (20f). Brownish solid (89% yield, 170 mg). R_f 0.82 (50% EtOAc/hexanes); ^{1}H NMR (DMSO-d_6, 300MHz) δ 8.99 (s, 1H), 8.57 (s, 1H), 7.90 (d, *J* = 8.70, 2H), 7.58 (d, *J* = 8.70, 2H), 7.36 (d, *J* = 9.00, 2H), 6.88 (d, *J* = 9.30, 2H), 3.93 (t, *J* = 6.60, 2H), 2.49 (s, 3H), 1.71–1.66 (m, 2H), 1.42–1.28 (m, 10H), 0.88–0.84 (m, 3H); HRMS *m/z* 382.2271 (calcd for $C_{23}H_{30}N_2O_3$, 382.2256); Anal. Calcd for $C_{23}H_{30}N_2O_3$ (382.22): C, 72.22; H, 7.91; N, 7.32; found: C, 72.43; H, 8.00; N, 7.48.

4.1.3.7. 1-(4-Acetylphenyl)-3-(4-(nonyloxy)phenyl)urea (20g). Brownish solid (77% yield, 153 mg). R_f 0.84 (50% EtOAc/hexanes); ^{1}H NMR (DMSO-d_6, 300MHz) δ 8.99 (s, 1H), 8.57 (s, 1H),7.90 (d, *J* = 8.70, 2H), 7.58 (d, *J* = 8.40, 2H), 7.36 (d, *J* = 9.00, 2H), 6.88 (d, *J* = 9.30, 2H), 3.93 (t, *J* = 6.60, 2H), 2.49 (s, 3H), 1.70–1.65 (m, 2H), 1.42–1.25(m, 12H), 0.87–0.83 (m, 3H); HRMS *m/z* 396.2400 (calcd for $C_{24}H_{32}N_2O_3$, 396.2413); Anal. Calcd for $C_{24}H_{32}N_2O_3$ (396.24): C, 72.70; H, 8.13; N, 7.06; found: C, 72.91; H, 8.20; N, 7.29.

4.1.3.8. 1-(4-Acetylphenyl)-3-(4-isobutoxyphenyl)urea (20h). Off-white solid (80% yield, 130 mg). R_f 0.73 (50% EtOAc/hexanes); ^{1}H NMR (DMSO-d_6, 300MHz) δ9.05 (s, 1H), 8.63 (s, 1H),7.90 (d, *J* = 8.70, 2H), 7.58 (d, *J* = 8.70, 2H), 7.36 (d, *J* = 7.80, 2H), 6.88 (d, *J* = 8.70, 2H), 3.70 (d, *J* = 6.60, 2H), 2.49 (s, 3H), 1.99–1.95 (m, 1H), 0.98 (d, *J* = 6.60, 6H HRMS *m/z* 326.1632 (calcd for $C_{19}H_{22}N_2O_3$,

326.1630); Anal. Calcd for $C_{19}H_{22}N_2O_3$ (326.16): C, 69.92; H, 6.79; N, 8.58; found: C, 70.13; H, 6.85; N, 8.74.

4.1.3.9. 1-(4-Acetylphenyl)-3-(4-(isopentyloxy)phenyl)urea (20i). Off-white solid (75% yield, 128 mg). R_f 0.75 (50% EtOAc/hexanes); ^{1}H NMR (DMSO-d_6, 300MHz) δ 8.99 (s, 1H), 8.57 (s, 1H),7.90 (d, *J* = 8.70, 2H), 7.58 (d, *J* = 8.70, 2H), 7.36 (d, *J* = 9.00, 2H), 6.88 (d, *J* = 9.00, 2H), 3.93 (t, *J* = 6.60, 2H), 2.49 (s, 3H), 1.74–1.69 (m, 2H), 1.66–1.64 (m, 1H), 1.33–1.28 (m, 2H), 0.90 (d, *J* = 6.60, 6H); HRMS *m/z* 340.1780 (calcd for $C_{20}H_{24}N_2O_3$, 340.1787); Anal. Calcd for $C_{20}H_{24}N_2O_3$ (340.17): C, 70.57; H, 7.11; N, 8.23; found: C, 70.79; H, 7.15; N, 8.42.

4.1.3.10. 1-(4-Acetylphenyl)-3-(4-((4-methylpentyl)oxy)phenyl)urea (20j). Off-white solid (92% yield, 162 mg). R_f 0.75 (95% EtOAc/hexanes); ^{1}H NMR (DMSO-d_6, 300MHz) δ8.99 (s, 1H), 8.57 (s, 1H),7.90 (d, *J* = 8.70, 2H), 7.58 (d, *J* = 8.70, 2H), 7.36 (d, *J* = 9.00, 2H), 6.88 (d, *J* = 9.00, 2H), 3.93 (t, *J* = 6.60, 2H), 2.49 (s, 3H), 1.74–1.69 (m, 2H), 1.66–1.64 (m, 1H), 1.33–1.28 (m, 2H), 0.90 (d, *J* = 6.60, 6H); HRMS *m/z* 354.1953 (calcd for $C_{21}H_{26}N_2O_3$, 354.1943); Anal. Calcd for $C_{21}H_{26}N_2O_3$ (354.19): C, 71.16; H, 7.39; N, 7.90; found: C, 71.43; H, 7.44; N, 8.06.

4.1.3.11. 1-(4-Acetylphenyl)-3-(4-(2-ethylbutoxy)phenyl)urea (20k). Off-white solid (82% yield, 145 mg). R_f 0.71 (50% EtOAc/hexanes); ^{1}H NMR (DMSO-d_6, 300MHz) δ 9.01 (s, 1H), 8.59 (s, 1H),7.90 (d, *J* = 8.70, 2H), 7.56 (d, *J* = 8.40, 2H), 7.36 (d, *J* = 8.40, 2H), 6.89 (d, *J* = 8.40, 2H), 3.82 (d, *J* = 5.40, 2H), 2.49 (s, 3H), 1.62–1.56 (m, 1H), 1.66–1.64 (m, 1H), 1.47–1.31 (m, 4H), 0.92–0.85 (m, 6H); HRMS *m/z* 354.1949 (calcd for $C_{21}H_{26}N_2O_3$, 354.1943); Anal. Calcd for $C_{21}H_{26}N_2O_3$ (354.19): C, 71.16; H, 7.39; N, 7.90; found: C, 71.44; H, 6.84; N, 8.03.

4.1.3.12. 1-(4-Acetylphenyl)-3-(4-(cyclobutylmethoxy)phenyl)urea (20l). Off-white solid (78% yield, 132 mg). R_f 0.76 (50% EtOAc/hexanes); ^{1}H NMR (DMSO-d_6, 300MHz) δ8.99 (s, 1H), 8.57 (s, 1H),7.90 (d, *J* = 8.70, 2H), 7.58 (d, *J* = 9.00, 2H), 7.36 (d, *J* = 8.70, 2H), 6.88 (d, *J* = 9.40, 2H), 3.91 (d, *J* = 6.60, 2H), 2.61–2.76 (m, 1H), 2.49 (s, 3H), 2.16–2.64 (m, 2H), 1.81–1.89 (m, 4H); ^{13}C NMR (DMSO-d_6) δ 196.19, 154.27, 152.27, 144.51, 132.14, 130.21, 129.58, 120.24, 116.96, 114.66, 71.71, 34.04,

24.35, 18.05; HRMS *m/z* 338.1650 (calcd for $C_{20}H_{22}N_2O_3$, 338.1630); Anal. Calcd for $C_{20}H_{22}N_2O_3$ (338.16): C, 70.99; H, 6.55; N, 8.28; found: C, 71.15; H, 6.64; N, 8.44.

4.1.3.13. 1-(4-Acetylphenyl)-3-(4-(cyclopentyloxy)phenyl)urea (20m). Off-white solid (65% yield, 110 mg). R_f 0.8 (50% EtOAc/hexanes); ^{1}H NMR (DMSO-d_6, 300MHz) δ 9.05 (s, 1H), 8.61 (s, 1H),7.90 (d, *J* = 8.10, 2H), 7.58 (d, *J* = 8.40, 2H), 7.35 (d, *J* = 9.00, 2H), 6.85 (d, *J* = 8.40, 2H), 4.75 (br s, 1H), 2.49 (s, 3H), 1.88–1.56 (m, 8H); HRMS *m/z* 338.1628 (calcd for $C_{20}H_{22}N_2O_3$, 338.1630); Anal. Calcd for $C_{20}H_{22}N_2O_3$ (338.16): C, 70.99; H, 6.55; N, 8.28; found: C, 71.24; H, 6.53; N, 8.41.

4.1.3.14. 1-(4-Acetylphenyl)-3-(4-(cycloheptyloxy)phenyl)urea (20n). Brownish white solid (68% yield, 125 mg). R_f 0.85 (50% EtOAc/hexanes); ^{1}H NMR (DMSO-d_6, 300MHz) δ9.6 (s, 1H), 9.16 (s, 1H), 7.89 (d, *J* = 8.10, 2H), 7.60 (d, *J* = 8.10, 2H), 7.37 (d, *J* = 8.40, 2H), 6.84 (d, *J* = 8.40, 2H), 4.41–4.39 (br m, 1H), 2.49 (s, 3H), 1.95–1.89 (m, 2H), 1.79–1.44 (m, 10H); HRMS *m/z* 366.1938 (calcd for $C_{22}H_{26}N_2O_3$, 366.1943); Anal. Calcd for $C_{22}H_{26}N_2O_3$ (366.19): C, 72.11; H, 7.15; N, 7.64; found: C, 72.40; H, 7.21; N, 7.80.

4.1.3.15. 1-(4-Acetylphenyl)-3-(4-(benzyloxy)phenyl)urea (20o).[40] Off-white solid (97% yield, 175 mg). R_f 0.91 (50% EtOAc/hexanes); ^{1}H NMR (DMSO-d_6, 300MHz) δ9.02 (s, 1H), 8.06 (s, 1H), 7.90 (d, *J* = 8.70, 2H), 7.58 (d, *J* = 8.70, 2H), 7.45–7.32(m, 7H), 6.97 (d, *J* = 8.10, 2H), 5.10 (s, 2H), 2.49 (s, 3H); HRMS *m/z* 360.1463 (calcd for $C_{22}H_{20}N_2O_3$, 360.1474); Anal. Calcd for $C_{22}H_{20}N_2O_3$ (360.14): C, 73.32; H, 5.59; N, 7.77; found: C, 73.56; H, 5.26; N, 7.78.

4.1.4. Preparation of Carbamimidoylhydrazono Derivatives 17 and 21a-o. General Procedures. The methyl ketones (**17** and **19**, 0.5 mmol) were dissolved in absolute ethanol (10 mL), and aminoguanidine hydrochloride (111 mg, 1 mmol) and a catalytic amount of LiCl (10 mg) were added. The reaction mixture was heated under reflux for 12-24 hours. The solvent was evaporated under reduced pressure. The crude product was purified by crystallization from 70% methanol, then recystalization again from ethyl acetate to afford the final products as listed below:

4.1.4.1. 2-{1-[4-(3-(4-(*tert*-Butyl)phenyl)ureido)phenyl]ethylidene}hydrazine-1-carboximidamide (17). Buff solid (76%): mp > 300 °C. ^{1}H NMR (DMSO-d_6) δ 9.70 (brs, 1 H), 8.60 (brs, 1 H), 7.72 (d, *J* = 8.7 Hz, 2 H), 7.41 (d, *J* = 8.7 Hz, 2 H), 7.37 (d, *J* = 8.7 Hz, 2 H), 7.27 (d, *J* = 8.7 Hz, 2 H), 5.83 (brs, 2 H), 5.43 (brs, 2 H), 2.19 (s, 3 H), 1.24 (s, 9 H); ^{13}C NMR (DMSO-d_6, 100MHz) δ 160.20, 153.41, 148.19, 145.02, 140.08, 137.97, 134.64, 126.82, 126.28, 119.00, 118.39, 34.78, 32.17, 14.20; ESIMS *m/z* (rel intensity) 367 ([M+H]$^+$, 100); HRMS (ESI), *m/z* 367.2252 M$^+$, calcd for $C_{20}H_{27}N_6O$ 367.2241.

4.1.4.2. 2-(1-(4-(3-(4-Propoxyphenyl)ureido) phenyl)ethylidene) hydrazine-1-carboximidamide (21a). Yellowish solid (80% yield, 147 mg). R_f 0.5 (DCM/MeOH/Et_3N, 87:10:3); ^{1}H NMR (DMSO-d_6, 300MHz) δ11.20(s, 1H), 9.69(s, 1H), 9.48 (s, 1H), 7.91 (br s, 3H), 7.39 (d, *J* = 8.70, 2H), 7.54 (d, *J* = 8.70, 2H), 7.42 (d, *J* = 8.70, 2H), 6.6.77 (d, *J* = 8.70, 2H), 3.84 (t, *J* = 6.60, 2H), 2.24 (s, 3H), 1.71–1.64 (m, 2H), 0.97 (t, *J* = 7.50, 3H); ^{13}C NMR (DMSO-d_6, 100MHz) δ 156.49, 154.04, 153.22, 151.96, 142.34, 133.54, 130.22, 127.63, 120.34, 117.77, 114.88, 72.56, 23.49, 14.47, 10.68; HRMS *m/z* 368.1980 (calcd for $C_{19}H_{24}N_6O_2$, 368.1961); Anal. Calcd for $C_{19}H_{24}N_6O_2$ (368.19): C, 61.94; H, 6.57; N, 22.81; found: C, 62.13; H, 6.66; N, 23.06.

4.1.4.3. 2-(1-(4-(3-(4-Butoxyphenyl)ureido)phenyl)ethylidene)hydrazine-1-carboximidamide (21b). Yellowish solid (82% yield, 157 g). R_f 0.51 (DCM/MeOH/Et_3N, 87:10:3); ^{1}H NMR (DMSO-d_6, 300MHz) δ 9.90 (s, 1H), 9.56 (s, 1H),7.86 (d, *J* = 8.70, 2H), 7.84 (br s, 3H), 7.49 (d, *J* = 8.70, 2H), 7.35 (d, *J* = 9.00, 2H), 6.88 (d, *J* = 8.70, 2H), 4.68 (s, 1H), 3.89 (t, *J* = 6.30, 2H), 2.31(s, 3H), 1.68–1.63 (m, 2H), 1.44–1.40 (m, 2H), 0.94 (t, *J* = 7.20, 3H); ^{13}C NMR (DMSO-d_6, 100MHz) δ 156.42, 153,70, 152.81, 151.05, 141.63, 132.79, 129.74, 127.34, 119.47, 116.81, 114.58, 67.26, 30.80, 18.69, 14.45, 13.66; HRMS *m/z* 382.2121 (calcd for $C_{20}H_{26}N_6O_2$, 382.2117); Anal. Calcd for $C_{20}H_{26}N_6O_2$ (382.21): C, 62.81; H, 6.85; N, 21.97; found: C, 63.07; H, 6.92; N, 22.14.

4.1.4.4. 2-(1-(4-(3-(4-(Pentyloxy)phenyl)ureido)phenyl)ethylidene)hydrazine-1 carboximidamide (21c). Yellowish solid (75% yield, 148 mg). R_f 0.54 (DCM/MeOH/Et_3N, 87:10:3); ^{1}H NMR (DMSO-d_6,

300MHz) δ11.01 (s, 1H), 9.45 (s, 1H), 9.21 (s, 1H), 7.80 (d, *J* = 8.40, 2H), 7.75 (br s, 3H), 7.53 (d, *J* = 8.70, 2H), 7.39 (d, *J* = 8.40, 2H), 6.80 (d, *J* = 8.70, 2H), 3.87 (t, *J* = 6.30, 2H), 2.26 (s, 3H), 1.69–1.62 (m, 2H), 1.39–1.29 (m, 4H), 0.91–0.86 (m, 3H); ^{13}C NMR (DMSO-d_6, 100MHz) δ 155.88, 153,71, 152.69, 151.57, 141.83, 132.87, 129.66, 127.23, 119.92, 117.23, 114.42, 67.53, 28.43, 27.70, 21.86, 14.01, 13.85; HRMS *m/z* 396.2282 (calcd for $C_{21}H_{28}N_6O_2$, 396.2274); Anal. Calcd for $C_{21}H_{28}N_6O_2$ (396.22): C, 63.62; H, 7.12; N, 21.20; found: C, 63.80; H, 7.21; N, 21.49.

4.1.4.5. 2-(1-(4-(3-(4-(Hexyloxy)phenyl)ureido)phenyl)ethylidene)hydrazine-1-carboximidamide (21d). Yellowish white solid (62% yield, 127 mg). R_f 0.56 (DCM/MeOH/Et_3N, 87:10:3);^{1}H NMR (DMSO-d_6, 300MHz) δ 9.04 (s, 1H), 8.62 (s, 1H),7.90 (d, *J* = 8.70, 2H), 7.58 (d, *J* = 8.40, 2H), 7.36 (d, *J* = 8.10, 2H), 6.88 (d, *J* = 8.70, 2H), 3.93 (t, *J* = 6.30, 2H), 2.49 (s, 3H), 1.70–1.64 (m, 2H), 1.40–1.29 (m, 6H), 0.87–0.85 (m, 3H); ^{13}C NMR (DMSO-d_6, 100MHz) δ 155.89, 153,64, 152.69, 151.56, 141.90, 132.94, 129.59, 127.18, 119.88, 117.24, 114.33, 67.50, 30.98, 28.70, 25.16, 21.99, 13.81 (2C); HRMS *m/z* 410.2432 (calcd for $C_{22}H_{30}N_6O_2$, 410.2430); Anal. Calcd for $C_{22}H_{30}N_6O_2$ (410.24): C, 64.37; H, 7.37; N, 20.47; found: C, 64.51; H, 7.41; N, 20.70.

4.1.4.6. 2-(1-(4-(3-(4-(Heptyloxy)phenyl)ureido)phenyl)ethylidene)hydrazine-1-carboximidamide (21e). Yellowish white solid (88% yield, 187 g). R_f 0.57 (DCM/MeOH/Et_3N, 87:10:3); ^{1}H NMR (DMSO-d_6, 300MHz) δ 11.15 (br s, 1H), 9.52 (s, 1H), 9.30 (s, 1H), 7.58 (d, *J* = 8.70, 2H), 7.71 (br s, 3H), 7.52 (d, *J* = 8.70, 2H), 7.40 (d, *J* = 8.70, 2H), 6.79 (d, *J* = 9.00, 2H), 3.88 (t, *J* = 6.30, 2H), 2.25 (s, 3H), 1.69–1.62 (m, 2H), 1.38–1.27 (m, 8H), 0.88–0.84 (m, 3H); HRMS *m/z* 424.2600 (calcd for $C_{23}H_{32}N_6O_2$, 424.2587); Anal. Calcd for $C_{23}H_{32}N_6O_2$ (424.25): C, 65.07; H, 7.60; N, 19.80; found: C, 65.31; H, 7.69; N, 20.03.

4.1.4.7. 2-(1-(4-(3-(4-(octyloxy)phenyl)ureido)phenyl)ethylidene)hydrazine-1-carboximidamide (21f). Yellowish white solid (80% yield, 175 mg). R_f 0.58 (DCM/MeOH/Et_3N, 87:10:3); ^{1}H NMR (DMSO-d_6, 300MHz) δ 11.02 (brs, 1H),)9.72 (s, 1H), 9.45 (s, 1H),7.77 (d, *J* = 9.00, 2H), 7.45 (d, *J* = 9.00, 2H), 7.38 (d, *J* = 8.70, 2H), 6.84 (d, *J* = 9.00, 2H), 6.76 (br s, 3H), 3.91 (t, *J* = 6.60 Hz, 2H), 2.25

(s, 3H), 1.72–1.63 (m, 2H), 1.39–1.26 (m, 10H), 0.85–0.83 (m, 3H); ^{13}C NMR (DMSO-d_6, 100MHz) δ 156.44, 154.12, 153.19, 151.98, 142.32, 133.46, 130.18, 127.64, 120.37, 117.74, 114.82, 67.98, 31.70, 29.25, 29.12, 26.02, 22.53, 14.46, 14.40; HRMS *m/z* 438.2731 (calcd for $C_{24}H_{34}N_6O_2$, 438.2743); Anal. Calcd for $C_{24}H_{34}N_6O_2$ (438.27): C, 65.73; H, 7.81; N, 19.16; found: C, 66.01; H, 7.89; N, 19.44.

4.1.4.8. 2-(1-(4-(3-(4-(nonyloxy)phenyl)ureido)phenyl)ethylidene)hydrazine-1-carboximidamide (21g). Pale yellow solid (70% yield, 158 g). R_f 0.6 (DCM/MeOH/Et_3N, 87:10:3); ^{1}H NMR (DMSO-d6, 300MHz) δ11.10 (br s, 1H), 9.55 (s, 1H), 9.32 (s, 1H), 7.84 (br s, 3H), 7.76 (d, *J* = 8.40, 2H), 7.53 (d, *J* = 8.10, 2H), 7.40 (d, *J* = 8.70, 2H), 6.77 (d, *J* = 8.70, 2H), 3.87 (t, *J* = 6.60, 2H), 2.25 (s, 3H), 1.68–1.63 (m, 2H), 1.37–1.25(m, 12H), 0.87–0.83 (m, 3H); ^{13}C NMR (DMSO-d_6, 100MHz) δ 156.36, 154.08, 153.20, 152.10, 142.42, 133.52, 130.07, 127.66, 120.36, 117.75, 114.77, 67.96, 31.74, 29.44, 29.31, 29.27, 29.14, 26.02, 22.55, 14.45, 14.39; HRMS *m/z* 452.2893 (calcd for $C_{25}H_{36}N_6O_2$, 452.2900); Anal. Calcd for $C_{25}H_{36}N_6O_2$ (452.29): C, 66.34; H, 8.02; N, 18.57; found: C, 66.59; H, 8.13; N, 18.81.

4.1.4.9. 2-(1-(4-(3-(4-isobutoxyphenyl)ureido)phenyl)ethylidene)hydrazine-1-carboximidamide (21h). Yellow solid (65% yield, 0124 mg). R_f 0.48 (DCM/MeOH/Et_3N, 87:10:3); ^{1}H NMR (DMSO-d6, 300MHz) δ 11.12 (br s, 1H), 9.58 (s, 1H), 9.35 (s, 1H), 7.85 (br s, 3H), 7.76 (d, *J* = 7.80, 2H), 7.53 (d, *J* = 7.80, 2H), 7.41(d, *J* = 7.50, 2H), 6.79 (d, *J* = 8.10, 2H), 3.65 (d, *J* = 5.70, 2H), 2.25 (s, 3H), 1.98–1.94 (m, 1H), 0.96 (d, *J* = 6.30, 6H); ^{13}C NMR (DMSO-d_6, 100MHz) δ 155.92, 153.73, 152.74, 151.63, 141.95, 133.08, 129.60, 127.17, 119.90, 117.30, 114.39, 73.93, 27.71, 19.01, 13.97; HRMS *m/z* 382.2125 (calcd for $C_{20}H_{26}N_6O_2$, 382.2117); Anal. Calcd for $C_{20}H_{26}N_6O_2$ (382.21): C, 62.81; H, 6.85; N, 21.97; found: C, 63.07; H, 6.92; N, 22.14.

4.1.4.10. 2-(1-(4-(3-(4-(Isopentyloxy)phenyl)ureido)phenyl)ethylidene)hydrazine-1-carboximidamide (21i). Yellow solid (60% yield, 119 mg). R_f 0.5 (DCM/MeOH/Et_3N, 87:10:3); ^{1}H NMR (DMSO-d_6, 300MHz) δ 11.12 (br s, 1H), 9.52 (s, 1H), 9.28 (s, 1H), 7.84 (br s, 3H), 7.79 (d, *J* = 8.40, 2H), 7.54 (d, *J* = 8.10, 2H), 7.40 (d, *J* = 8.40, 2H), 6.80 (d, *J* = 8.40, 2H), 3.92 (t, *J* = 6.00, 2H), 2.26 (s, 3H), 1.78–1.71 (m, 1H), 1.59–1.1.54 (m, 2H), 0.92 (d, *J* = 6.30, 6H); ^{13}C NMR (DMSO-d_6, 100MHz)

δ 155.89, 153.68, 152.72, 151.61, 141.91, 132.95, 129.61, 127.22, 119.94, 117.25, 114.39, 65.96, 37.52, 24.54, 22.39, 13.99; HRMS *m/z* 396.2260 (calcd for $C_{21}H_{28}N_6O_2$, 396.2274); Anal. Calcd for $C_{21}H_{28}N_6O_2$ (396.22): C, 63.62; H, 7.12; N, 21.20; found: C, 63.84; H, 7.19; N, 21.47.

4.1.4.11. 2-(1-(4-(3-(4-((4-methylpentyl)oxy)phenyl)ureido)phenyl)ethylidene)hydrazine-1-carboximid-amide (21j). Faint yellow solid (90% yield, 185 mg). R_f 0.51 (DCM/MeOH/Et_3N, 87:10:3); ^{1}H NMR (DMSO-d6, 300MHz) δ11.12 (br s, 1H), 9.50 (s, 1H), 9.24 (s, 1H), 7.80 (m, 5H), 7.53 (d, *J* = 8.40, 2H), 7.39 (d, *J* = 9.00, 2H), 6.79 (d, *J* = 9.00, 2H), 3.88 (t, *J* = 6.60, 2H), 2.26 (s, 3H), 1.69–1.63 (m, 2H), 1.64–1.54 (m, 1H), 1.31–1.25 (m, 2H), 0.88 (d, *J* = 6.60, 6H) ; ^{13}C NMR (DMSO-d_6, 100MHz) δ 155.92, 153.69, 152.69, 151.52, 141.82, 132.88, 129.67, 127.20, 119.90, 117.22, 114.40, 67.82, 34.68, 27.23, 26.65, 22.38, 13.99; HRMS *m/z* 410.2444 (calcd for $C_{22}H_{30}N_6O_2$, 410.2430); Anal. Calcd for $C_{22}H_{30}N_6O_2$ (410.24): C, 64.37; H, 7.37; N, 20.47; found: C, 64.64; H, 7.45; N, 20.70.

4.1.4.12. 2-(1-(4-(3-(4-(2-Ethylbutoxy)phenyl)ureido)phenyl)ethylidene)hydrazine-1-carboximidamide (21k). Yellowish white solid (85% yield, 174 mg). R_f 0.52 (DCM/MeOH/Et_3N, 87:10:3); ^{1}H NMR (DMSO-d_6, 300MHz) δ 11.21 (brs, 1H), 9.53 (s, 1H), 9.24 (brs, 1H), 7.95 (brs, 3H),7.81 (d, *J* = 8.70, 2H), 7.56 (d, *J* = 8.40, 2H), 7.36 (d, *J* = 8.40, 2H), 6.80 (d, *J* = 8.40, 2H), 3.82 (d, *J* = 5.40, 2H), 2.38 (s, 3H), 1.62–1.56 (m, 1H), 1.47–1.31 (m, 4H), 0.92–0.85 (m, 6H); ^{13}C NMR (DMSO-d_6, 100MHz) δ 156.39, 154.43, 153.18, 151.91, 142.31, 133.32, 130.10, 127.80, 120.28, 117.59, 114.98, 70.21, 23.26, 14.61, 11.42, 10.88; HRMS *m/z* 410.2439 (calcd for $C_{22}H_{30}N_6O_2$, 410.2430); Anal. Calcd for $C_{22}H_{30}N_6O_2$ (410.24): C, 64.37; H, 7.37; N, 20.47; found: C, 64.55; H, 7.48; N, 20.71.

4.1.4.13. 2-(1-(4-(3-(4-(Cyclobutylmethoxy)phenyl)ureido)phenyl)ethylidene)hydrazine-1-carboximid-amide (21l). yellow solid (66% yield, 130 mg). R_f 0.49 (DCM/MeOH/Et_3N, 87:10:3); ^{1}H NMR (DMSO- d_6, 300MHz) δ 9.97 (s, 1H), 9.65 (s, 1H), 7.96 (brs, 3H), 7.87 (d, *J* = 8.10, 2H), 7.49 (d, *J* = 8.40, 2H), 7.35 (d, *J* = 8.40, 2H), 6.85 (d, *J* = 8.70, 2H), 4.68 (brs, 1 H), 3.88 (d, *J* = 6.90, 2 H), 2.71–2.66 (m, 1 H), 2.31 (s, 3H), 2.03–1.99 (m, 2H), 1.81–1.76 (m, 4H); HRMS *m/z* 394.2131 (calcd for

$C_{21}H_{26}N_6O_2$, 394.2117); Anal. Calcd for $C_{21}H_{26}N_6O_2$ (394.21): C, 63.94; H, 6.64; N, 21.30; found: C, 64.13; H, 6.74; N, 21.56.

4.1.4.14. 2-(1-(4-(3-(4-(Cyclopentyloxy)phenyl)ureido)phenyl)ethylidene)hydrazine-1-carboximidamide (20m). Yellowish solid (58% yield, 114g). R_f 0.51 (DCM/MeOH/Et_3N, 87:10:3); ^{1}H NMR (DMSO-d_6, 300MHz) δ 9.82 (s, 1H), 9.49 (s, 1H), 8.91 (brs, 1H), 7.87 (d, *J* = 8.40 Hz, 2 H), 7.82 (brs, 1 H), 7.50 (d, *J* = 8.10, 2H), 7.34 (d, *J* = 8.70 Hz, 2 H), 7.27 (brs, 2 H), 6.82 (d, *J* = 9.00, 2H), 4.77 (s, 1H), 2.31 (s, 3 H), 1.86–1.56 (m, 8 H); ^{13}C NMR (DMSO-d_6, 100MHz) δ 159.79, 156.70, 153.27, 153.07, 142.21, 133.08, 130.06, 127.90, 120.05, 117.27, 116.10, 79.16, 32.68, 24.00, 14.96; HRMS *m/z* 394.2130 (calcd for $C_{21}H_{26}N_6O_2$, 394.2117); Anal. Calcd for $C_{21}H_{26}N_6O_2$ (394.21): C, 63.94; H, 6.64; N, 21.30; found: C, 64.12; H, 6.69; N, 21.54.

4.1.4.15. 2-(1-(4-(3-(4-(Cycloheptyloxy)phenyl)ureido)phenyl)ethylidene)hydrazine-1-carboximidamide (21n). Brownish yellow solid (84% yield, 177 mg). R_f 0.56 (DCM/MeOH/Et_3N, 87:10:3); ^{1}H NMR (DMSO-d6, 300MHz) δ 11.10 (br s, 1H), 9.55 (s, 1H), 9.32 (s, 1H), 7.80 (br s, 3H), 7.77 (d, *J* = 8.10, 2H), 7.53 (d, *J* = 8.40, 2H), 7.39 (d, *J* = 8.70, 2H), 6.76 (d, *J* = 8.70, 2H), 4.36–4.34 (m, 1H), 2.25 (s, 3H), 1.94–1.87 (m, 2H), 1.69–1.42 (m, 10H); ^{13}C NMR (DMSO-d_6, 100MHz) δ 156.37, 153.21, 152.68, 151.99, 142.40, 133.37, 130.07, 127.70, 120.45, 117.68, 116.47, 77.55, 33.62, 28.33, 22.80, 14.50; HRMS *m/z* 422.2440 (calcd for $C_{23}H_{30}N_6O_2$, 422.2430); Anal. Calcd for $C_{23}H_{30}N_6O_2$ (422.24): C, 65.38; H, 7.16; N, 19.89; found: C, 65.54; H, 7.23; N, 20.04.

4.1.4.16. 2-(1-(4-(3-(4-(Benzyloxy)phenyl)ureido)phenyl)ethylidene)hydrazine-1-carboximidamide (21o). Yellowish brown solid (90% yield, 187 g). R_f 0.62 (DCM/MeOH/Et_3N, 87:10:3); ^{1}H NMR (DMSO-d6, 300MHz) δ 11.12 (brs, 1H), 9.54 (s, 1H), 9.32 (s, 1H), 7.83 (br s, 3H), 7.79 (d, *J* = 8.40, 2H), 7.54 (d, *J* = 8.40, 2H), 7.36–1.24 (m, 7H), 6.90 (d, *J* = 8.40, 2H), 5.00 (s, 2H), 2.26 (s, 3H); ^{13}C NMR (DMSO-d_6, 100MHz) δ 155.94, 153.32, 152.71, 151.52, 141.81, 137.25, 133.29, 129.71, 128.30, 127.63, 127.56, 127.21, 119.88, 117.27, 114.82, 69.39, 13.99; HRMS *m/z* 416.1954

(calcd for $C_{23}H_{24}N_6O_2$, 416.1961); Anal. Calcd for $C_{23}H_{24}N_6O_2$ (416.19): C, 66.33; H, 5.81; N, 20.18; found: C, 66.91; H, 5.97; N, 20.72.

4.2. MICROBIOLOGICAL ASSAYS

4.2.1. Determination of Minimum Inhibitory Concentration (MIC) and Minimum Bactericidal Concentration (MBC). MRSA clinical isolates (NRS119 and NRS123) and VRSA strains (VRS10, VRS11a, and VRS12) were obtained through the Network of Antimicrobial Resistance in *Staphylococcus aureus* (NARSA) program and BEI Resources.

The MICs of the newly synthesized compounds, tested against isolates of *S. aureus*, were determined using the broth microdilution method in accordance with the Clinical and Laboratory Standards Institute guidelines.[41] Bacteria were cultured in cation-adjusted Mueller Hinton broth in a 96-well plate. Compounds, using triplicate samples, were added to the plate and serially diluted. Plates were incubated at 37 °C for 20 hours prior to determining the MIC. Plates were visually inspected and the MIC was categorized as the concentration at which no visible growth of bacteria was observed. The average of triplicate MIC determinations is reported. The MBC was determined by transferring a small aliquot (5 uL), from wells where no growth was observed (in the MIC plates), onto Tryptic soy agar plates. Plates were incubated at 37 °C for at least 18 hours prior to determining the MBC; the MBC was categorized as the lowest concentration where 99.9% of bacterial growth was inhibited.

4.2.2. Time-kill assay of diphenylurea compounds against MRSA. MRSA USA400 cells in logarithmic growth phase (OD_{600} = 0.796) were diluted to 9.20×10^5 colony-forming units (CFU/mL) and exposed to concentrations equivalent to 4 × MIC (in triplicate) of compounds **21i**, **21n**, **21j** and vancomycin in Tryptic soy broth. Aliquots (100 µL) were collected from each treatment after 0, 2, 4, 6, 8, 10, 12, and 24 hours of incubation at 37 °C and subsequently serially diluted in PBS. Bacteria were then transferred to Tryptic soy agar plates and incubated at 37 °C for 18-20 hours before viable CFU/mL was determined.

4.2.3. *In vitro* cytotoxicity analysis of diphenylurea compounds against HaCaT cells. Compounds **21d**, **21h**, **21c**, **21i**, **21a**, **21n**, and **21j** were assayed (at concentrations of 8, 16, 32, and 64 µg/mL) against a human keratinocyte (HaCaT) cell line (Catalogue Number: T0020001, AddexBio, San Diego, CA, USA) to determine the potential toxic effect to mammalian skin cells *in vitro*. Briefly, cells were cultured in Dulbecco's Modified Eagle Medium (DMEM) supplemented with 10% fetal bovine serum (FBS) at 37 °C with CO_2 (5%). Control cells received DMSO alone at a concentration equal to that in drug-treated cell samples. The cells were incubated with the compounds (in triplicate) in a 96-well plate at 37 ºC with CO_2 (5%) for two hours. The assay reagent MTS 3-(4,5-dimethylthiazol-2-yl)-5-(3-carboxymethoxyphenyl)-2-(4-sulfophenyl)-2*H*-tetrazolium) (Promega, Madison, WI, USA) was subsequently added and the plate was incubated for four hours. Absorbance readings (at OD_{490}) were taken using a kinetic microplate reader (Molecular Devices, Sunnyvale, CA, USA). The quantity of viable cells after treatment with each compound was expressed as a percentage of the viability of DMSO-treated control cells (average of triplicate wells ± standard deviation). The toxicity data was analyzed via a one-way ANOVA, with post hoc Dunnet's multiple comparisons test ($P < 0.05$), utilizing GraphPad Prism 6.0 (GraphPad Software, La Jolla, CA).

4.2.4. Intracellular infection of J774 cells with MRSA and treatment with diphenylurea compound 21n. ***Toxicity assessment***: Compounds **21i** and **21n** were assayed (at concentrations of 8, 16, 32, and 64 µg/mL) against a murine macrophage (J774) cell line to determine the potential toxic effect *in vitro*. Briefly, cells were cultured in Dulbecco's Modified Eagle Medium (DMEM) supplemented with 10% FBS at 37 °C with CO_2 (5%). Control cells received DMSO alone at a concentration equal to that in drug-treated cell samples. The cells were incubated with the compounds (in triplicate) in a 96-well plate at 37 ºC with CO_2 (5%) for 24 hours. The assay reagent MTS 3-(4,5-dimethylthiazol-2-yl)-5-(3-carboxymethoxyphenyl)-2-(4-sulfophenyl)-2*H*-tetrazolium) (Promega, Madison, WI, USA) was subsequently added and the plate was incubated for four hours. Absorbance readings (at OD_{490}) were taken using a kinetic microplate reader (Molecular Devices, Sunnyvale, CA, USA). The quantity of viable

cells after treatment with each compound was expressed as a percentage of the viability of DMSO-treated control cells (average of triplicate wells ± standard deviation). The toxicity data was analyzed via a one-way ANOVA, with post hoc Dunnet's multiple comparisons test ($P < 0.05$), utilizing GraphPad Prism 6.0 (GraphPad Software, La Jolla, CA).

4.2.5. ***Eradication of intracellular MRSA***: Murine macrophage cells (J774) were cultured in Dulbecco's Modified Eagle Medium (DMEM) supplemented with 10% FBS at 37 °C with CO_2 (5%). J774 cells were exposed to MRSA USA400 cells at a multiplicity of infection of approximately 100:1. One-hour post-infection, J774 cells were washed with gentamicin (50 µg/mL) to kill extracellular MRSA. Compound **21n** and vancomycin, at a concentration equal to 16 µg/mL, were added. At specified time points (4, 8, and 24 hours), the test agents were removed; J774 cells were washed with gentamicin (50 µg/mL) and subsequently lysed using 0.1% Triton-X 100. The solution was serially diluted in phosphate-buffered saline and transferred to Tryptic soy agar plates in order to enumerate the viable number of MRSA colony-forming units (CFU) present inside the J774 cells. Plates were incubated at 37 ºC for 18-22 hours before counting viable CFU/mL. Data are presented as percent reduction of MRSA USA400 CFU/mL in infected J774 cells in relation to the untreated control. The data was analyzed via a t-test ($P < 0.05$), utilizing GraphPad Prism 6.0 (GraphPad Software, La Jolla, CA). Asterisks (*) indicate statistical significance between compound **21n** and vancomycin.

4.2.6. Detecting if compounds exert their antibacterial activity by physically disrupting the bacterial cell membrane. In order to investigate the effect of the lead compound on the integrity of the bacterial cell envelope, the release of 260 and 280 nm absorbing components was determined spectrophotometrically. The cell suspension of 2.52×10^9 CFU/mL MRSA NRS123 (USA400) was incubated with 5.0 × MIC of compounds **21i**, **21n**, or vancomycin at 37 °C for 30 minutes. For the complete release of 260 and 280 nm absorbing material (nucleic acids, proteins, etc.), the bacterial suspension (control) was treated with lysostaphin (20 µg/mL in 50 mM Tris-HCl, pH 7.6) for 30 minutes. The absorbance of cell supernatant at 260 and 280 nm was determined using a spectrophotometer

(Jenway 6305, Staffordshire, UK). The average OD_{260} and OD_{280} values of duplicates for each treatment option were calculated and expressed as the proportion of average OD_{260} (or OD_{280}) for each treatment option compared to the average OD_{260} (or OD_{280}) for the positive control (lysostaphin-treated cells).

4.2.7. *In vivo* examination of 21n and vancomycin to kill MRSA USA400 in a *Caenorhabditis elegans* animal model. To examine the efficacy of the diphenylurea compounds to treat a MRSA infection *in vivo*, the animal model *Caenorhabditis elegans* (*C. elegans*) was utilized as described elsewhere.[42] The temperature-sensitive sterile mutant strain *C. elegans* AU37 [sek-1(km4); glp-4(bn2) I] was used as this strain is sterile at room temperature and capable of laying eggs only at 15 °C. Additionally, this strain is more susceptible to infection due to a mutation in the *sek-1* gene of the p38 mitogen-activated protein kinase pathway. Briefly, worms were grown for five days at 15 °C (permitting adult worms to lay eggs) on nematode growth medium (NGM) agar plates seeded with a lawn of *Escherichia coli* (*E. coli*) OP50. The eggs were harvested by bleaching and maintained for 24 hours at room temperature with gentle agitation for hatching. Hatched larvae were transferred to a new NGM plate seeded with *Escherichia coli* OP50 and were kept at room temperature for 4-5 days until worms reached the adult stage of growth (L4). Adult worms were collected and washed three times with PBS in a 1:10 ratio to remove *E. coli*.

To test the antibacterial activity of the diphenylurea compounds against MRSA *in vivo*, adult worms were transferred to TSA agar plates seeded with a lawn of MRSA USA400 for infection. After six hours of infection, worms were collected and washed with M9 buffer three times before transferring 15-25 worms to wells in a 96-well microtiter plate. Worms were incubated with 10 µg/mL of tested compound, vancomycin (positive control), or PBS (negative control) (in triplicate). Worms were monitored to ensure compounds did not exhibit adverse toxicity. After treatment for 20 hours, worms were washed three times with M9 buffer and then examined microscopically to examine morphological changes and viability. They were subsequently lysed in microcentrifuge tubes containing 200 mg of 1.0-mm silicon carbide particles (Biospec Products, Bartlesville, OK) that were vortexed for one minute. Samples were serially

diluted and plated onto TSA plates containing 5 µg/mL nalidixic acid to select for MRSA growth. Plates were incubated at 37 °C for 18 hours before viable CFU was determined. MRSA USA400 CFU was divided by the number of worms receiving each treatment to determine MRSA USA400 CFU per worm for each treatment group. A Student's t-test (with Holm-Sidak correction) was utilized to determine statistical significance ($P < 0.05$) in CFU/worm for treated groups relative to the untreated control.

4.3. PHARMACOKINETICS PROFILING

4.3.1. Permeability analysis for compound 21n. Caco-2 cells were grown in tissue culture flasks, trypsinized, suspended in medium, and known concentration of cell suspensions were seeded onto wells of a Millipore 96-well Caco-2 plate. The cells were allowed to grow and differentiate for three weeks, feeding at two-day intervals. For apical to basolateral (A→B) permeability, the test article was added to the apical (A) side and amount of permeation on the basolateral (B) side was determined; for basolateral to apical (B→A) permeability, the test article was added to the B side and the amount of permeation on the A side was determined. To test tight junctions and monolayer integrity, the A-side buffer contained 100 µM Lucifer yellow dye in Transport Buffer (1.98 g/L glucose in 10 mM HEPES, 1x Hank's Balanced Salt Solution) with pH 6.5 while the B-side buffer was Transport Buffer with pH 7.4. Caco-2 cells were incubated with these buffers for two hours, and the receiver side buffer was removed for analysis by LC/MS/MS. To verify the tight junctions and integrity of Caco-2 cell monolayers, aliquots of the cell buffers were analyzed by fluorescence (Lucifer yellow transport ≤ 2%). Any deviations from control values are reported. Data are expressed as permeability (P_{app}) = $(dQ/dt)/(C_0A)$ where dQ/dt is the rate of permeation, C_0 is the initial concentration of test agent, and A is the area of the monolayer. In bidirectional permeability studies, the Efflux Ratio (Re) is also calculated: $R_e = (P_{app}\ B\rightarrow A)/ (P_{app}\ A\rightarrow B)$; $R_e > 2$ indicates a potential substrate for P-glycoprotein or other active efflux transporter(s).

4.3.2. Metabolic stability analysis. The tested compounds were incubated in duplicate with pooled human liver microsomes at 37 ºC. The reaction contained microsomal protein in 100 mM potassium phosphate buffer (pH 7.4), 2 mM NADPH, and 3 mM $MgCl_2$. A control was run for each test article

omitting NADPH to detect NADPH-free degradation. At predetermined time points, an aliquot was removed from each experimental and control reaction and mixed with an equal volume of ice-cold methanol containing propranolol as the internal standard to stop the reaction and precipitate proteins. Stopped reactions were kept on ice for at least ten minutes followed by an addition of equal volume of water. The samples were centrifuged to remove precipitated protein, and the supernatants were analyzed by LC-MS/MS to quantify parent remaining. Data was calculated as % parent remaining by assuming zero-minute time point peak area ratio (analyte/IS) as 100% and dividing remaining time point peak area ratios by the zero-minute time point peak area ratio. Data was subjected to fit a first-order decay model to calculate slope and thereby half-life. Intrinsic clearance was calculated from the half-life and the human liver microsomal protein concentrations using the following equations:

CL_{int} = ln(2) /($T_{1/2}$ [microsomal protein]); $T_{1/2}$ = 0.693/-k; CL_{int} = intrinsic clearance; $T_{1/2}$ = half-life; k = slope.

4.3.3. ***In Vivo*** **Pharmacokinetics.** This assay has been conducted at a credited bioequivalence center (http://www.grc-me.com/pk_pd.html). Pharmacokinetic studies were performed in male naïve Sprague−Dawley (SD) rats, (three animals) following Institutional Animal Care and Use Committee guidelines. Oral dosing (50 mg/kg) was administered by gavage in a vehicle containing 5% ethanol, 45% PEG 400, and 50% water. Blood samples were collected over a 24 hour period post dose into Vacutainer tubes containing EDTA-K2. Plasma was isolated, and the concentration of compound **21n** in plasma was determined with LC/MS/MS after protein precipitation with acetonitrile.

Non-compartmental pharmacokinetic analysis was performed on plasma concentration data to calculate pharmacokinetic parameters using Kinetica® 2000 (release 4.4.1).

Acknowledgements. This research is supported by Deanship of Scientific Research, University of Dammam, Project # 2014177. The authors would like to thank BEI Resources, NIAID, and NIH for clinical isolates of *S. aureus* used in this study.

Associated Contents

Supporting Information. Synthetic schemes of all hit compounds and their precursors, their characterization data in addition to copies of all NMR spectra. This material is available free of charge via the Internet at http://pubs.acs.org.

Author Contributions

‖ These two authors contributed equally.

References

[1] D.M. Brogan, E. Mossialos, A critical analysis of the review on antimicrobial resistance report and the infectious disease financing facility, Global. Health, 12 (2016).

[2] J. O'NEILL, Tackling Drug-Resistant Infections Globally: final report and recommendations, *Rev. Antimicrob. Resist*., (2016) http://amr-review.org/Publications.

[3] T. Tada, B. Shrestha, T. Miyoshi-Akiyama, K. Shimada, H. Ohara, T. Kirikae, B.M. Pokhrel, NDM-12, a novel New Delhi metallo-beta-lactamase variant from a carbapenem-resistant *Escherichia coli* clinical isolate in Nepal, *Antimicrob. Agents Chemother*., 58 (2014) 6302-6305.

[4] X. Yao, Y. Doi, L. Zeng, L. Lv, J.H. Liu, Carbapenem-resistant and colistin-resistant Escherichia coli co-producing NDM-9 and MCR-1, *Lancet Infect Dis*, 16 (2016) 288-289.

[5] H. de Lencastre, D. Oliveira, A. Tomasz, Antibiotic resistant *Staphylococcus aureus*: a paradigm of adaptive power, *Curr. Opin. Microbiol.*, 10 (2007) 428-435.

[6] M.P. Jevons, "Celbenin" - resistant Staphylococci, *Br Med J*, 1 (1961) 124-125.

[7] M. Barber, M. Rozwadowska-Dowzenko, Infection by penicillin-resistant staphylococci, *Lancet*, 2 (1948) 641-644.

[8] J.E. Peacock, Jr., F.J. Marsik, R.P. Wenzel, Methicillin-resistant *Staphylococcus aureus*: introduction and spread within a hospital, *Ann. Intern. Med.*, 93 (1980) 526-532.

[9] K. Crossley, B. Landesman, D. Zaske, An outbreak of infections caused by strains of *Staphylococcus aureus* resistant to methicillin and aminoglycosides. II. Epidemiologic studies, *J. Infect. Dis.*, 139 (1979) 280-287.

[10] Peter Wilson, J. A. Andrews, R. Charlesworth, R. Walesby, M. Singer, D. J. Farrell, M. Robbins, Linezolid resistance in clinical isolates of *Staphylococcus aureus*, *J. Antimicrob. Chemother.*, 51 (2003) 186-188.

[11] K. Hiramatsu, Vancomycin-resistant Staphylococcus aureus: a new model of antibiotic resistance, *Lancet Infect. Dis.*, 1 (2001) 147-155.

[12] C. Hawkins, J. Huang, N. Jin, G.A. Noskin, T.R. Zembower, M. Bolon, Persistent *Staphylococcus aureus* bacteremia: an analysis of risk factors and outcomes, *Arch. Intern. Med.*, 167 (2007) 1861-1867.

[13] R. Khatib, L. Johnson, M. Sharma, M. Fakih, R. Ganga, K. Riederer, Persistent *Staphylococcus aureus* bacteremia: incidence and outcome trends over time, Scand. *J. Infect. Dis.*, 41 (2009) 4-9.

[14] J.C. Dombrowski, L.G. Winston, Clinical failures of appropriately-treated methicillin-resistant Staphylococcus aureus infections, *J. Infect.*, 57 (2008) 110-115.

[15] T.P. Lodise, B. Lomaestro, J. Graves, G.L. Drusano, Larger vancomycin doses (at least four grams per day) are associated with an increased incidence of nephrotoxicity, *Antimicrob. Agents Chemother.*, 52 (2008) 1330-1336.

[16] G. Wang, J.F. Hindler, K.W. Ward, D.A. Bruckner, Increased vancomycin MICs for Staphylococcus aureus clinical isolates from a university hospital during a 5-year period, *J. Clin. Microbiol.*, 44 (2006) 3883-3886.

[17] H. Mohammad, A.S. Mayhoub, M. Cushman, M.N. Seleem, Anti-biofilm activity and synergism of novel thiazole compounds with glycopeptide antibiotics against multidrug-resistant staphylococci, *J. Antibiot.*, 68 (2015) 259-266.

[18] H. Mohammad, A.S. Mayhoub, A. Ghafoor, M. Soofi, R.A. Alajlouni, M. Cushman, M.N. Seleem, Discovery and characterization of potent thiazoles versus methicillin- and vancomycin-resistant *Staphylococcus aureus*, *J. Med. Chem.*, 57 (2014) 1609-1615.

[19] H. Mohammad, P.V. Reddy, D. Monteleone, A.S. Mayhoub, M. Cushman, G.K. Hammac, M.N. Seleem, Antibacterial Characterization of Novel Synthetic Thiazole Compounds against Methicillin-Resistant *Staphylococcus pseudintermedius*, *PloS One*, 10 (2015) e0130385.

[20] H. Mohammad, P.V. Reddy, D. Monteleone, A.S. Mayhoub, M. Cushman, M.N. Seleem, Synthesis and antibacterial evaluation of a novel series of synthetic phenylthiazole compounds against methicillin-resistant *Staphylococcus aureus* (MRSA), *Eur. J. Med. Chem.*, 94 (2015) 306-316.

[21] M.A. Seleem, A.M. Disouky, H. Mohammad, T.M. Abdelghany, A.S. Mancy, S.A. Bayoumi, A. Elshafeey, A. El-Morsy, M.N. Seleem, A.S. Mayhoub, Second-Generation Phenylthiazole Antibiotics with Enhanced Pharmacokinetic Properties, *J Med Chem*, 59 (2016) 4900-4912.

[22] ZINC PAINS patterns search; http://zinc15.docking.org/patterns/home.

[23] R. Loewe, S. Lociuro, S. Hawser, L. Schmitt, Diphenyl urea derivatives, in, Google Patents, 2010.

[24] L. Garuti, M. Roberti, G. Bottegoni, M. Ferraro, Diaryl Urea: A Privileged Structure in Anticancer Agents, *Curr. Med. Chem.*, 23 (2016) 1528-1548.

[25] M. Ekroos, T. Sjogren, Structural basis for ligand promiscuity in cytochrome P450 3A4, *Proc. Natl. Acad. Sci. U. S. A.*, 103 (2006) 13682-13687.

[26] Y. Cheng, F. Zhang, T.A. Rano, Z. Lu, W.A. Schleif, L. Gabryelski, D.B. Olsen, M. Stahlhut, C.A. Rutkowski, J.H. Lin, L. Jin, E.A. Emini, K.T. Chapman, J.R. Tata, Indinavir analogues with blocked metabolism sites as HIV protease inhibitors with improved pharmacological profiles and high potency against PI-resistant viral strains, *Bioorg. Med. Chem. Lett.*, 12 (2002) 2419-2422.

[27] Z.K. Wan, E. Chenail, J. Xiang, H.Q. Li, M. Ipek, J. Bard, K. Svenson, T.S. Mansour, X. Xu, X. Tian, V. Suri, S. Hahm, Y. Xing, C.E. Johnson, X. Li, A. Qadri, D. Panza, M. Perreault, J.F. Tobin, E. Saiah, Efficacious 11beta-hydroxysteroid dehydrogenase type I inhibitors in the diet-induced obesity mouse model, *J Med. Chem.*, 52 (2009) 5449-5461.

[28] S.R. Singh, A.E. Bacon, 3rd, D.C. Young, K.A. Couch, In vitro 24-hour time-kill studies of vancomycin and linezolid in combination versus methicillin-resistant Staphylococcus aureus, *Antimicrob. Agents Chemother.*, 53 (2009) 4495-4497.

[29] L. Cantoni, M.P. Glauser, J. Bille, Comparative efficacy of daptomycin, vancomycin, and cloxacillin for the treatment of *Staphylococcus aureus* endocarditis in rats and role of test conditions in this determination, *Antimicrob Agents Chemother*, 34 (1990) 2348-2353.

[30] D.P. Levine, B.S. Fromm, B.R. Reddy, Slow response to vancomycin or vancomycin plus rifampin in methicillin-resistant *Staphylococcus aureus* endocarditis, *Ann. Intern. Med.*, 115 (1991) 674-680.

[31] P. Vergidis, M.S. Rouse, G. Euba, M.J. Karau, S.M. Schmidt, J.N. Mandrekar, J.M. Steckelberg, R. Patel, Treatment with linezolid or vancomycin in combination with rifampin is effective in an animal model of methicillin-resistant Staphylococcus aureus foreign body osteomyelitis, *Antimicrob Agents Chemother*, 55 (2011) 1182-1186.

[32] E. Brouillette, G. Grondin, L. Shkreta, P. Lacasse, B.G. Talbot, In vivo and in vitro demonstration that Staphylococcus aureus is an intracellular pathogen in the presence or absence of fibronectin-binding proteins, *Microbial pathogenesis*, 35 (2003) 159-168.

[33] F.D. Lowy, Is *Staphylococcus aureus* an intracellular pathogen?, *Trends Microbiol*, 8 (2000) 341-343.

[34] M. Cruciani, G. Gatti, L. Lazzarini, G. Furlan, G. Broccali, M. Malena, C. Franchini, E. Concia, Penetration of vancomycin into human lung tissue, *J Antimicrob Chemoth*, 38 (1996) 865-869.

[35] S.M. Lehar, T. Pillow, M. Xu, L. Staben, K.K. Kajihara, R. Vandlen, L. DePalatis, H. Raab, W.L. Hazenbos, J.H. Morisaki, J. Kim, S. Park, M. Darwish, B.C. Lee, H. Hernandez, K.M. Loyet, P. Lupardus, R. Fong, D. Yan, C. Chalouni, E. Luis, Y. Khalfin, E. Plise, J. Cheong, J.P. Lyssikatos, M. Strandh, K. Koefoed, P.S. Andersen, J.A. Flygare, M. Wah Tan, E.J. Brown, S. Mariathasan, Novel antibody-antibiotic conjugate eliminates intracellular *S. aureus*, *Nature*, 527 (2015) 323-328.

[36] P.A. Moise-Broder, A. Forrest, M.C. Birmingham, J.J. Schentag, Pharmacodynamics of vancomycin and other antimicrobials in patients with *Staphylococcus aureus* lower respiratory tract infections, *Clin. Pharmacokinet*, 43 (2004) 925-942.

[37] T.I. Moy, A.R. Ball, Z. Anklesaria, G. Casadei, K. Lewis, F.M. Ausubel, Identification of novel antimicrobials using a live-animal infection model, *Proc. Natl. Acad. Sci. U. S. A.*, 103 (2006) 10414-10419.

[38] R.A. Alajlouni, M.N. Seleem, Targeting listeria monocytogenes rpoA and rpoD genes using peptide nucleic acids, *Nucleic Acid Ther.*, 23 (2013) 363-367.

[39] M.L. Landrum, C. Neumann, C. Cook, U. Chukwuma, M.W. Ellis, D.R. Hospenthal, C.K. Murray, Epidemiology of Staphylococcus aureus blood and skin and soft tissue infections in the US military health system, 2005-2010, *JAMA*, 308 (2012) 50-59.

[40] J.-Y. Winum, F. Carta, C. Ward, P. Mullen, D. Harrison, S.P. Langdon, A. Cecchi, A. Scozzafava, I. Kunkler, C.T. Supuran, Ureido-substituted sulfamates show potent carbonic anhydrase IX inhibitory and antiproliferative activities against breast cancer cell lines, *Bioorg. Med. Chem. Lett.*, 22 (2012) 4681-4685.

[41] Clinical and Laboratory Standards Institute (2012) Methods for Dilution Antimicrobial Susceptibility Tests for Bacteria That Grow Aerobically—Ninth Edition: Approved Standard M07-A9. Wayne, PA.

[42] T. Stiernagle, Maintenance of C. elegans, WormBook : the online review of C. elegans biology, (2006) 1-11.

- Diphenylurea is a promising class of antibiotics with anti-MRSA activity
- Adding a *para*-alkoxy side chain enhances the metabolic stability
- The cycloheptyl **21n** has balanced PD/PK and toxicological properties